

# Accepted Manuscript

Design, synthesis and biological evaluation of thiosemicarbazones, hydrazinobenzothiazoles and arylhydrazones as anticancer agents with a potential to overcome multidrug resistance

Veronika F.S. Pape, Szilárd Tóth, András Füredi, Kornélia Szebényi, Anna Lovrics, Pál Szabó, Michael Wiese, Gergely Szakács

PII: S0223-5234(16)30261-6

DOI: [10.1016/j.ejmech.2016.03.078](https://doi.org/10.1016/j.ejmech.2016.03.078)

Reference: EJMECH 8503

To appear in: *European Journal of Medicinal Chemistry*

Received Date: 9 December 2015

Revised Date: 22 March 2016

Accepted Date: 25 March 2016

Please cite this article as: V.F.S. Pape, S. Tóth, A. Füredi, K. Szebényi, A. Lovrics, P. Szabó, M. Wiese, G. Szakács, Design, synthesis and biological evaluation of thiosemicarbazones, hydrazinobenzothiazoles and arylhydrazones as anticancer agents with a potential to overcome multidrug resistance, *European Journal of Medicinal Chemistry* (2016), doi: 10.1016/j.ejmech.2016.03.078.

This is a PDF file of an unedited manuscript that has been accepted for publication. As a service to our customers we are providing this early version of the manuscript. The manuscript will undergo copyediting, typesetting, and review of the resulting proof before it is published in its final form. Please note that during the production process errors may be discovered which could affect the content, and all legal disclaimers that apply to the journal pertain.



**Design, synthesis and biological evaluation of thiosemicarbazones, hydrazinobenzothiazoles and arylhydrazones as anticancer agents with a potential to overcome multidrug resistance**

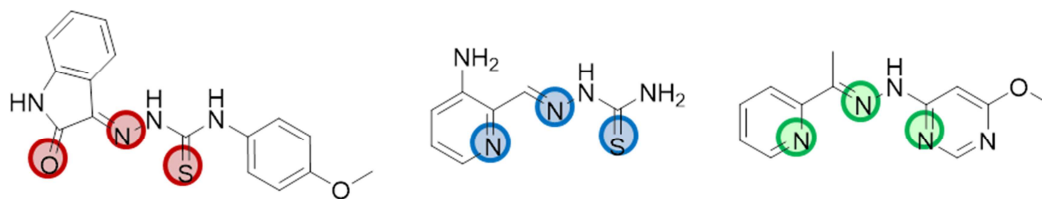
Veronika F.S. Pape,<sup>[a,b]</sup> Szilárd Tóth,<sup>[a]</sup> András Füredi,<sup>[a]</sup> Kornélia Szebényi,<sup>[a]</sup> Anna Lovrics,<sup>[a]</sup> Pál Szabó,<sup>[c]</sup> and Michael Wiese,<sup>\*[b]</sup> Gergely Szakács<sup>\*[a]</sup>

[a] Institute of Enzymology, Research Centre for Natural Sciences, Hungarian Academy of Sciences, Budapest, Hungary

[b] Department of Pharmaceutical Chemistry, University of Bonn, Bonn, Germany

[c] Dr. P. Szabó, Institute of Organic Chemistry, Research Centre for Natural Sciences, Hungarian Academy of Sciences, Budapest, Hungary

\* corresponding authors: szakacs.gergely@ttk.mta.hu (GSz), mwiese@uni-bonn.de (MW)

**Graphical abstract**

**Keywords:** Antitumor agents • Cancer • Chelators • Multidrug Resistance • Schiff bases

**Abbreviations**

ABC, ATP-binding cassette; APT, attached proton test; DMEM, Dulbecco's Modified Eagle medium; HSAB, hard and soft acids and bases; MMP, matched molecular pair; MTT, 3-(4,5-dimethylthiazol-2-yl)-2,5-diphenyltetrazolium bromide; PBS, phosphate buffered saline; P-gp, P-glycoprotein; RPMI, Roswell Park Memorial Institute; RR, ribonucleotide reductase; TQ, Tariquidar; TSC, thiosemicarbazone.

Supporting information for this article is given via a link at the end of the document.

**Abstract:** There is a constant need for new therapies against multidrug resistant (MDR) cancer. An attractive strategy is to develop chelators that display significant antitumor activity in multidrug resistant cancer cell lines overexpressing the drug efflux pump P-glycoprotein. In this study we used a panel of sensitive and MDR cancer cell lines to evaluate the toxicity of picolinylidene and salicylidene thiosemicarbazone, arylhydrazones, picolinylidene and salicylidene hydrazino-benzothiazole derivatives. Our results confirm the collateral sensitivity of MDR cells to isatin- $\beta$ -thiosemicarbazones, and identify several chelator scaffolds with a potential to overcome multidrug resistance. Analysis of structure-activity-relationships within the investigated compound library indicates that NNS and NNN donor chelators show superior toxicity as compared to ONS derivatives regardless of the resistance status of the cells.

## 1. Introduction

Cancer is the second highest cause of death in industrialized countries [1,2]. Currently a broad range of diverse compounds with different mechanisms of anticancer activity is available for treatment [3]. Despite the diversity of drugs, cancer often proves incurable due to the development of drug resistance [2]. Moreover, cancer cells that develop resistance against a single cytotoxic agent show cross-resistance to structurally and mechanistically unrelated drugs [3]. Multidrug resistance (MDR) can emerge as a result of reduced uptake or increased efflux of cytostatic agents – the latter is mediated by ATP-binding-cassette (ABC) proteins, primarily by P-glycoprotein (P-gp), which confers resistance to a wide variety of compounds [3–7]. There is a constant need for novel chemotherapeutics with marked and selective antitumor activity that can overcome resistance to established therapies.

The increased proliferation of cancer cells results in an elevated demand for metal ions, which creates a vulnerability that can be exploited therapeutically [8–11]. The toxicity of chelators is

mediated by the perturbation of intracellular metal homeostasis, the formation of redox active complexes, which generate reactive oxygen species (ROS), or the inhibition of metalloproteins such as ribonucleotide reductase (RR) [8,12,13]. Several chelators targeting cell-cycle progression and DNA synthesis have been reported as potentially active anticancer agents [9,12–15]. Since the first report of the moderate antileukemic activity of 2-formyl thiosemicarbazone in 1956 [16], the chemical space around thiosemicarbazones (TSCs) with anticancer activity has been explored intensely. The most investigated TSC is Triapine, a tridentate  $\alpha$ -*N*-pyridyl thiosemicarbazone (Figure 1, upper middle panel). Triapine is a potent RR inhibitor currently undergoing phase I and II clinical trials [17–19]. While the clinical efficacy of Triapine awaits confirmation, *in vitro* experiments have suggested that Triapine is subject to MDR, as it is recognized and transported by P-gp [20,21]. Substitution on the terminal nitrogen (N4) of the TSC moiety was reported to increase toxicity of TSC derivatives [21–23]. The terminally dimethylated TSC di-2-pyridylketone-4,4,-dimethyl-3-thiosemicarbazone (Dp44mT, Figure 1, upper middle panel) has even been shown to exhibit a paradoxical hypertoxicity against the P-gp-overexpressing cervix carcinoma cell line KB-V1 as compared to its parental cell line KB-3-1 [8,24]. In order to circumvent transporter mediated resistance, inhibiting the transporters appeared to be a valuable approach [25–33]. Despite promising *in vitro* results, successful translation of MDR transporter inhibition to the clinic remains elusive [25,34–38]. Compounds showing increased toxicity against MDR cells represent a promising strategy to overcome resistance in cancer [39]. The analysis of NCI's Developmental Therapeutics Program (DTP) drug screening data has led to the identification of a series of “MDR-selective” compounds whose toxicity was positively correlated with P-gp expression across the NCI60 cells representing tumor types of different tissue origins [40–42]. The toxicity of MDR-selective compounds is indeed paradoxically increased in P-gp-expressing MDR cells and is abrogated in the presence of P-gp inhibitors [15,40], revealing

that in contrast to the export of toxic substrates, P-gp can directly sensitize MDR cells [15,21,40,43]. Interestingly, the structurally diverse MDR-selective compounds share the ability to chelate metal ions. In particular, there is a strong link between the thiosemicarbazone backbone and MDR selective toxicity, as exemplified by several isatin- $\beta$ -thiosemicarbazones including NSC73306 (**1a**, Figure 1, upper left panel), NSC658339, NSC716765, NSC716766, NSC716768, NSC716771 and NSC716772 (for structures, see Table S1) [15,21,40,43,44]. In addition to these TSCs the pharmacogenomic approach also identified a benzothiazole (NSC693630, Figure 1, upper middle panel) as a candidate MDR-selective agent [15]. The pyrimidinylhydrazone VP035 (Figure 1, upper right panel) has been reported to show selective toxicity towards MDR cell lines, yet in a P-gp independent manner [13].

In this study we characterize the anticancer activity of compounds designed around these five chelators possessing variable MDR-selective toxicity. The MDR-selective isatin- $\beta$ -thiosemicarbazone **1a** (NSC73306) is an ONS donor chelator, Dp44mT and Triapine are NNS donor chelators; the benzothiazole NSC693630 is able to bind metal ions via an NNS or NNN coordination mode [15], and the arylhydrazone VP035 is an NNN donor chelator [13,45,46].

In particular, our aim was to explore the chemical space around these compounds with regard to toxicity and MDR selectivity (Figure 1). We designed a focused library containing picolinylidene TSCs (class II), salicylidene TSCs (class III), in which respective chemical entities of the confirmed MDR-selective compounds (Figure 1, upper panels) are retained. To study derivatives of VP035, several *N*-hetero-arylhydrazones (class IV) were investigated. Picolinylidene (class V) and salicylidene (class VI) hydrazino-benzothiazoles were included in the library as derivatives of the hydrazino-benzothiazole NSC693630. Finally, various aspects of the chemical entities associated with MDR-selective activities were combined (class VII).

The compound library was tested for in vitro antiproliferative activity in six human cancer cell lines, including the drug sensitive and MDR ovarian carcinoma (A2780, A270adr), cervix carcinoma (KB-3-1, KB-V1) and uterine sarcoma (MES-SA, MES-SA/Dx5) cell lines.

## 2. Results

### 2.1. Design and synthesis of a focused chelator library

Several attempts have been made to elucidate the structural features that are responsible for the MDR-selective toxicity of isatin- $\beta$ -thiosemicarbazones. The current understanding of the structure activity relationship of MDR selective isatin- $\beta$ -TSCs suggests a beneficial effect of an aromatic moiety at N4 [21,39]. Similarly, introduction of a phenyl substituent to the N4 position has been shown to increase the toxicity of dipyridylketone TSCs to a comparable extent as terminal dimethylation [23,47]. In contrast to Dp44mT and NSC73306, the toxicity of the terminally unsubstituted NNS thiosemicarbazone Triapine is attenuated by P-gp [20,21,48].

The library consists of three TSC classes (I-III), all of which possess an aromatic moiety at N4. Since the current understanding of the SAR additionally suggests a beneficial effect of either electron withdrawing or donating groups in the *para* position of the aromatic ring for selective activity towards MDR cell lines [39,44], compounds with nitro, methyl, and methoxy groups in this position were included in the library (Figure 2).

In addition to the reported TSC compounds **1a** [15,21,40,43,44], the N4 *para* tolyl derivative **1c** [44] and the N4 *para* nitrophenyl derivative **1d** [44], we synthesized a new 5-trifluoromethoxyisatin derivative **1b**. The N4 *meta*-trifluoromethyl derivative **1e** was commercially available (box I in Figure 2). In order to investigate the effect of a terminal aromatic substitution of the TSC moiety on toxicity and MDR selectivity of related derivatives, picolinylidene TSCs (Class II) were prepared with the same terminal substituents

as present in the MDR selective isatin- $\beta$ -TSCs (**2f**, **2j**, box II in Figures 1, 2). Substitutions at the imino carbon have been suggested to affect the toxicity of Schiff bases [13,49–52]. Therefore we also included the corresponding methylated derivatives in our study (**2c**, **2g**, box II in Figures 1, 2). Additionally, the acetaniline derivative **2p** was prepared, which is an NNS-donor TSC like **2g**, but has an anilinic NH<sub>2</sub> instead of the ring-incorporated pyridinyl nitrogen. In order to increase the similarity of the new compounds to the MDR selective isatin- $\beta$ -TSC compounds, we retained the ONS donor set of the isatin TSCs by replacing the pyridine moieties with salicylic residues (**3b**, **3c**, box III in Figures 1, 2). As depicted in Scheme 1, thiosemicarbazones were obtained by an acid catalyzed Schiff base condensation of the particular thiosemicarbazide (**C-1**, **C-2**, or **C-3**) with the corresponding ketone, in good to moderate yields. **C-1** to **C-3** were prepared from the corresponding isothiocyanates upon reaction with hydrazine [44,53].

Arylhydrazones (class IV) and benzothiazoles (classes V, VI) have been introduced as alternatives to thiosemicarbazones, since TSCs exhibit pharmacological side effects due to the putative liberation of H<sub>2</sub>S during their metabolism [54,55]. Similar to thiosemicarbazones, these compound classes also provide the possibility to chelate metal ions, which has been suggested to be an important feature in their mechanism of action [13,45,46]. For a systematic comparison to the previous compounds (boxes II and III, Figures 1, 2), the respective picolinylidene (**5a**, **5b**, **5c**, box V, Figures 1, 2), acetaniline (**5d**) and salicylidene hydrazinobenzothiazoles (**6a**, **6b**, box VI, Figures 1, 2) were obtained by reacting the keto components with the commercially available 2-hydrazinobenzothiazole under the same acid catalyzed conditions as applied for the TSCs and provided the products in good yields (Scheme 1). As depicted in Figures 1 and 2, benzothiazoles can also chelate metal ions via an NNN binding mode, similar to arylhydrazones. The latter compound class has been suggested as yet another



alternative to overcome the metabolic instability of TSCs [55]. In order to include more NNN donors into the study, the previously reported arylhydrazones **4a-c** [13] were incorporated to the study and the commercially available arylhydrazones **4d-h** (box IV, Figure 1, 2) were purchased

To further increase the similarity of the newly designed compounds to **1a**, chemical entities were combined in the four compounds presented in box VII (Figure 2): in **7a** the non-isatin moiety of **1a** is dimerized. This compound was obtained by reaction of the 4-methoxyphenylisothiocyanat with a half-equimolar amount of hydrazine. Two compounds were prepared to combine the chemical entities of **1a** with the hydrazinobenzothiazole compound class. For these, either 4-methoxyphenylisothiocyanat or isatin were reacted with the hydrazinobenzothiazole, to provide compounds **7b** and **7c**, respectively. **7d** is an arylhydrazone, obtained in an acid catalyzed condensation of isatin and 4-hydrazinyl-6-methoxypyrimidine.

In addition to the synthesized compounds, the library was extended with further commercially available compounds (**1e**, **2a**, **2b**, **2d**, **2h**, **2i**, **2l**, **2m**, **2n**, **2o**, **3a**, **3d**, **3e**, **3f**, **3g**, **4d**, **4e**, **4f**, **4g**, **4h**, **6c**, **6d**, **6e**, **6f**, **6g**). For all compounds included in this study, the  $\log D_{7.4}$  values, total polar surface area (TPSA), as well as the strongest  $pK_a$  and  $pK_b$  values were predicted with the ChemAxon software [56] (Supplementary tables S2-S6).

## 2.2. Assessment of cytotoxicity in an MDR cell panel

The cytotoxic activity of the compounds was investigated in a panel of parental (sensitive) and MDR cancer cells. The ovarian carcinoma cell line A2780 and the uterine sarcoma cell line MES-SA were compared to their doxorubicin-selected counterparts A2780adr and MES-SA/Dx5, respectively [57–59], while the cervix carcinoma cell line KB-3-1 was compared to the vinblastine-selected line KB-V1 [60,61]. In addition, toxicity of selected active derivatives

was also evaluated in non-malignant HFF cells (Figure S1). As detailed in the experimental section, cytotoxicity of the compounds was measured using the MTT viability assay. In order to avoid a putative interaction of the investigated compounds with the assay reagent, the medium containing the test compound was removed before adding the reagent. Furthermore, no reaction could be observed in cell-free mixtures of compound solution and assay reagent. To exclude assay dependent results, MES-SA and MES-SA/Dx5 cells were engineered to stably express the mCherry fluorescent protein [62,63]. Therefore, the cell-killing effect of the test-compounds could additionally be investigated by fluorescent measurements avoiding putative side reactions with assay reagents [64]. As apparent from Figure S2, the two methods provided concordant results. Furthermore, Figure S2 highlights results obtained for hydroxyphenylhydrazone compounds, which have been reported to frequently disturb several diverse in vitro assays [65,66].

To identify whether the toxicity of the compounds is influenced by the activity of the multidrug transporter, the effect of the P-gp-inhibitor Tariquidar was also evaluated.

### 2.3. Confirmation of MDR selective activity of isatin- $\beta$ -thiosemicarbazones (**1a** – **1e**)

Figure 3 shows the differential effect of the P-gp-substrate Triapine and the MDR-selective compounds **1a** and **1d** in a cell line pair of MDR and parental cells. While the toxicity of Triapine is reduced by the transporter (Figure 3A), there is an increased sensitivity of the P-gp-positive MES-SA/Dx5 cells to **1a** (Figure 3B) and **1d** (Figure 3C) [44]. In the presence of the efflux pump inhibitor Tariquidar both resistance to Triapine and increased sensitivity to the MDR-selective compounds **1a** and **1d** are reverted to control levels measured in MES-SA cells. The fraction of IC<sub>50</sub> values obtained in P-gp negative vs. positive cells serves as a quantification of the MDR selective effect (selectivity ratio, SR). Figure 3D shows the SR values for the isatin- $\beta$ -thiosemicarbazones **1a** – **1e**. While the results of compound **1a** are in

good agreement with the literature [15,21,40,43,44], the magnitude of MDR selectivity of the N4 *para* tolyl derivative **1c** and the N4 *para* nitrophenyl derivative **1d** is much lower in our test system (compared to reported SR values of 9.2 for **1c** and 8.3 for **1d** [44]). In fact, **1c** is not selective in KB-V1 vs. KB-3-1 and A2780adr vs. A2780 cells.

According to our current understanding of the SAR of isatin- $\beta$ -thiosemicarbazones, substituents at the 5 position of the isatin moiety are tolerated, while *meta* substituents in the terminal phenyl ring have been described to have a detrimental effect on selective toxicity [39]. The two novel TSC derivatives, containing a trifluoromethoxygroup in the 5-position of the isatin moiety (as present in **1b**) or a trifluoromethyl substituent at the terminal phenyl ring (as present in **1e**) are consistent with this general conclusion (Figure 3D, Table S2). The P-gp inhibitor Tariquidar (TQ) abolished selectivity between the cell lines, proving that the cytotoxic activity of **1a**, **1b**, **1d** and **1e** is indeed potentiated by P-gp. Another characteristic of MDR-selective compounds is their ability to eliminate expression of P-gp and thus re-sensitize cells to chemotherapy [43]. Long-term exposure of MES-SA/Dx5 cells to compounds **1a**, **1c** or **1d** resulted in the elimination of P-gp-expressing cells, confirming the selective toxicity of these compounds to MDR cells (Figures 3 E-H, S2).

#### 2.4. Evaluation of selective toxicity in the compound library

After confirming the MDR-selective toxicity associated with the isatin- $\beta$ -thiosemicarbazone structures, we evaluated the activity of the compounds compiled in the focused library. As shown in Figures 1 and 2, the library combines several chemical motives that have been associated with MDR selective activity (such as the N4 substitution patterns and donor atom sets). The toxicity of the compounds was found to be similar across the cell lines, yielding IC<sub>50</sub> values in the submicromolar to micromolar range. Similarly to the parent compounds (**1a** – **1d**), several derivatives showed a significantly increased toxicity against some of the MDR

cells (Table 1). The picolinylidene TSC **2c** and the salicylidene benzothiazoles **6a** and **6b** were significantly more toxic to MES-SA/Dx5 than to MES-SA cells; **2g** showed selectivity in KB-V1 cells over KB-3-1; the arylhydrazones **4c** and **4b** showed selective activity in MES-SA/Dx5 over MES-SA cells as well as in A2780adr over A2780 cells [13]; the benzothiazoles **5b** and **5a**, as well as the salicylidene TSC **3a** showed selectivity in MES-SA/Dx5 over MES-SA cells (Tables 1, S2 - S6, Figures S2 - S6). It is striking that picolinylidene compounds containing a methyl group at the imino carbon (**2c**, **2g**, **4b**, **5b**) exhibit very high SR values. Yet, the selective toxicity of these compounds towards P-gp-expressing cells could not be confirmed in all of the MDR cell line pairs. Also in contrast to the isatin- $\beta$ -thiosemicarbazones, inhibition of P-gp did not abolish selectivity of these derivatives, suggesting that the hypersensitivity of the MDR cells to these compounds is not exclusively linked to P-gp.

### 2.5. Toxicity of picolinylidene Schiff bases in MES-SA and MES-SA/Dx5 cells

Based on studies with chloro- and methoxysubstituted derivatives, it has been suggested that substituents in the *para* position of the N4-phenyl group of isatin- $\beta$ -TSCs improve MDR selective toxicity, while the *meta* and *ortho* positions were found to be not beneficial [39,44]. As shown in Figure 4, various methyl substitutions at the N4-phenyl ring of picolinylidene TSCs follow the same trend: the toxicity on P-gp-negative MES-SA cells is similar for *ortho*- and *meta*-substituted picolinylidene TSC derivatives (**2i** and **2h**, respectively), but is reduced for the *para* tolyl TSC (**2g**). Conversely, in case of the P-gp-positive MES-SA/Dx5 cells the toxicity increases from *ortho*- (**2i**) to *meta*- (**2h**) to *para*-substituted (**2g**) derivatives. In case of trifluoromethyl substituents at the N4-phenyl ring the *ortho*-derivatives **2n** and **2o** were more toxic than the *meta*-substituted derivatives **2l** and **2m** in both investigated cell lines (the corresponding *para*-derivatives were unfortunately not available). The methyl and

trifluoromethyl substituted derivatives show a similar toxicity in case of *ortho* substitution (**2i** vs. **2o**), while in case of the *meta*-substituted derivatives, the tolyl TSC **2h** exhibits higher toxicity than the corresponding trifluoromethyl derivative **2m**. No strong correlation was found between the toxicity data of compounds presented in Figure 4 with calculated chemical properties (Table S7).

## 2.6. Effect of imino carbon methylation on the toxicity of the synthesized Schiff bases

Literature data suggest that the imino carbon of thiosemicarbazones [68], arylhydrazones [51], arylhydrazones [13] and benzothiazoles [49,50] may be a sensitive position for fine-tuning the biological activity of these Schiff bases. The role of imino carbon methylation on the toxicity of the investigated compounds is also evident from the structure-activity matrix shown in Figure 4. Figures 5A and B show the toxicity data of matched molecular pairs (MMPs) with and without imino carbon methylation. TSCs, benzothiazoles and arylhydrazones are shown with NNS (Figure 5A) and NNN (Figure 5B) donor atom sets. Introduction of a methyl group to the imino carbon results in increased toxicity in all investigated cell lines in two of the four investigated NNS donor MMPs (namely compounds **2f** vs. **2g** and **5a** vs. **5b**). For the N4-*ortho*-trifluoromethylphenyl TSC MMP, the imino-methylated derivative **2o** showed a higher toxicity than the desmethyl counterpart **2n** in MES-SA cells, while MES-SA/Dx5 cells reacted to both compounds with the same sensitivity. In the fourth MMP the methylated derivative **2m** was actually less toxic than the desmethyl derivative **2l**. In case of the NNN donor containing compounds, increased toxicity upon methylation could only be observed for the previously reported pyrimidinylhydrazone **4b** over **4a** [13], while toxicity of the arylhydrazones **4e** and **4g** was comparable to that of their respective imino carbon methylated derivatives **4f** and **4h** (Figures 4, 5 B). Increased toxicity of the imino methylated derivatives in MDR cells was observed in some, but not all

investigated cell line pairs (see Table 1, Figure S9 for more details). Extending the analysis to molecules without available MMPs showed that the activity of the imino carbon methylated picolinylidene compounds surpasses that of the unsubstituted derivatives (Figure 5 C). Together with the pairwise comparisons, these data suggest that methylation of the imino carbon may influence the toxicity of NNS donor atom chelators. In contrast, the three investigated MMPs with ONS donor atom sets did not show sensitivity to imino carbon methylation (see Figure S10).

### 2.7. Structure activity relationships

Even though the designed library did not provide new P-gp-dependent MDR-selective compounds, a systematic comparison of the cytotoxicity data allowed some conclusions concerning structure activity relationships as summarized in the structure activity matrix (SARM) shown in Figure 6 [69]. Our approach to combine chemical entities of the parent compounds shown in Figure 2 (box VII) mostly yielded compounds with modest cytotoxicity. Dimerization of the thiosemicarbazid moiety of **1a**, as present in compound **7a** did not show activity below 50  $\mu$ M. Combination of the thiosemicarbazone with the benzothiazole compound class resulted in compound **7b**, which was not cytotoxic at concentrations up to 50  $\mu$ M. Combining the benzothiazole with the isatin part of **1a** resulted in compound **7c**, which also lacked toxicity. Finally, combination of isatin with the arylhydrazone moiety produced a nontoxic compound (**7d**).

Comparison of the corresponding columns in the SARM shows that substitution of the phenyl moiety of TSCs results in lower toxicity of the N4-*para*-nitrophenyl derivatives as compared to *para*-tolyl and *para*-methoxyphenyl substituted counterparts (Figure 6, **1d** vs. **1a**, **1c**; **2j** vs. **2f**; **2k** vs. **2e**).

Hydrazinobenzothiazoles have been suggested to be superior to TSCs due to higher metabolic stability with retained pharmacologic activity [54]. Comparison of the corresponding columns in the SARM confirms the retained activity of the two scaffolds: the salicylidene-hydrazinobenzothiazole **6a** shows a similar toxicity than the corresponding TSC **3a**. Likewise, the picolinylidene-hydrazinobenzothiazole **5a** is comparable to the corresponding TSC **2a**.

### 2.8. Toxicity of hydrazino-benzothiazoles in MES-SA and MES-SA/Dx5 cells

Further derivatives of the benzothiazole class (see Figure 2, boxes V and VI) were investigated to evaluate the effect of substituents in *para* position to the chelating phenolic OH, which is predicted to influence the stability of formed metal complexes. The biological results of the hydrazinobenzothiazole series are summarized in Figure 7. In the methoxy-derivative of the salicylidene hydrazinobenzothiazole **6a** (**6g**) the ability to chelate is hindered, as one of the three donor atoms is occupied by the methyl group. Theoretically, this compound could bind metals via a bidentate chelation mode, but for steric reasons the expected complex stability would be rather low. Lack of toxicity of **6g** evidences the importance of chelation in the mechanism of toxicity. Introduction of an electron-donating methyl group (**6e**) or methoxy group (**6c** and **6d**) in *para* position to the metal binding hydroxyl group decreases the toxicity of the compounds. In contrast, the strong electron-withdrawing nitro group introduced at the same position increases toxicity (**6f**). In the case of the benzothiazoles there is a strong correlation of toxicity in both cell lines to the strongest calculated  $pK_b$  value, which is known to influence the metal binding ability of the ligand ( $r^2$  values 0.81 and 0.64 for MES-SA and MES-SA/Dx5 cells, respectively). Correlation with other chemical properties was not significant (Table S8). It is striking, that within this compound set the picolinylidene derivatives show an increased toxicity (box V, compounds **5a-c**) over salicylidene derivatives (box VI, compounds **6a-g**).

### 2.9. Influence of different donor atoms on chelator toxicity

Comparison of the rows within the SAR matrix offers an insight into the impact of different donor atom sets and the imino carbon substitution on toxicity of the compounds (Figure 6). In agreement with the observation on hydrazinobenzothiazoles, also the investigated salicylidene TSCs proved to be less toxic than their corresponding picolinylidene counterparts. Analysis of the matched molecular pairs (MMP) of ONS and NNS donors reveals a significant difference in toxicity across all investigated cell lines (Figure 8A). An extended analysis including compounds beyond the MMPs shown in Figure 8A confirms that chelators with an NNS or NNN donor set are significantly more toxic than the ONS chelators (Figure 5B, C). The  $pIC_{50}$  values measured in the sensitive and resistant cells are overall rather similar, confirming the lack of P-gp influence on the toxicity of these compounds (Figure 5C and S8).

Apart from the donor atoms alone, also steric factors will affect the ligands' ability to chelate a metal ion. The impact of these steric and electronic effects on the biological activity is evident from the comparison of the two investigated aniline derivatives **2p** and **5d** to their picolinylidene derivatives **2c** and **5b** (see SARM, Figure 6): the latter show a greater toxic potential.

### 2.10. Influence of donor atoms on drug activity patterns in the DTP database

In order to investigate whether the apparent difference in the toxicity of ONS and NNS donor chelators was restricted to compounds studied here, we performed substructure searches within the DTP database that contains the publically available toxicity profile of 40,000 compounds (Figures 9A, B and S9). Among the 1335 analogs identified in the DTP database (Figure S12), we found three MMPs with toxicity data on 60 cell lines (Figure 9C). Similarly



to the compounds investigated in the designed library, the 3 NNS chelators identified in the DTP set exhibited a higher toxic potential across the NCI-60 cell line panel than their respective ONS counterparts. Interestingly, the structurally related NSC95678, which is able to chelate in either binding mode, has a moderate toxicity between that of NNS and ONS chelators. Superior toxicity of the NNS donor set could also be observed on a larger set of NNS and ONS donor chelators but not in the subset of analogs that are not able to chelate metal ions (Figure 9D). Despite structural similarity, these compounds are unable to chelate because the putative donor atoms are either incorporated into ring systems or are otherwise occupied by substituents (examples are given in Figure S12). In this subset the toxicity of ONS and NNS compounds is similar, both being significantly less toxic than the chelators (Figure 9D).

### 3. Discussion

Chelators are widely investigated because of their therapeutic potential in the treatment of metal overload and diseases related to imbalanced metal homeostasis including hemochromatosis,  $\beta$ -thalassemia, Alzheimer's or Parkinson's diseases and cancer [8,9,12,70]. Several chelators display significant antitumor activity, and some were even shown to exhibit enhanced toxicity towards otherwise multidrug resistant cancer cell lines [13,15,21,40,43]. Increased sensitivity of MDR cancer cells suggested that P-glycoprotein may be an Achilles heel that can be targeted by MDR-selective compounds [15,39,40,43]. Our aim was to explore the chemical space around chelator classes such as the MDR selective isatin- $\beta$ -thiosemicarbazone **1a** or the P-gp-substrate pyridinyl TSC Triapine. A focused library was designed, allowing the systematic evaluation of different chelator scaffolds associated with MDR-

selective toxicity or multidrug resistance. *Para* substituted aromatic moieties that were identified to be associated with MDR selective toxicity in isatin- $\beta$ -thiosemicarbazone structures were attached to picolinylidene thiosemicarbazones (Figures 1, 2, box II). To further increase the similarity to the lead structure **1a**, the ONS donor atom set was retained in the salicylidene thiosemicarbazones (Figures 1, 2; box III). Finally, a series of hydrazinobenzothiazoles derivatives (Figures 1,2; boxes V, VI) were compared to respective TSCs analogs.

To evaluate the effect of P-gp on the compounds' activity (i.e. resistance or collateral sensitivity), we characterized the toxicity of the compounds in a panel of drug sensitive and MDR cell lines. In agreement with literature data, we find that Triapine is subject to MDR [20,21,48], while the isatin- $\beta$ -TSCs around **1a** show MDR-selective activity [15,21,40,43,44]. While most of the compounds studied here show comparable toxic potency in the investigated cell lines, some clearly target MDR cells (Tables 1, S2 - S6, Figures S2 - S6, S8, S10). In case of picolinylidene N4-tolyl thiosemicarbazones **2i**, **2h** and **2g**, the highest selectivity was achieved for the *para*-tolyl derivative **2g** in MES-SA/Dx5 vs. MES-SA cells. This is in agreement with studies on isatin- $\beta$ -TSCs, in which substituents in the *para* position of the N4-phenyl were shown to improve MDR-selective toxicity [39,44]. Cell line specific effects, that were independent of P-gp function, were observed for the picolinylidene TSC **2c**, the salicylidene TSC **3a**, the arylhydrazones **4c** and **4b**, the picolinylidene benzothiazoles **5b** and **5a**, as well as the salicylidene benzothiazoles **6a** and **6b** (Table 1). In case of the picolinylidene derivatives, compounds containing a methyl group at the imino carbon (**2c**, **2g**, **4b**, **5b**) show high selectivity ratios. The development of the MDR phenotype is a multifactorial process, and cell lines selected in toxins deploy several distinct mechanisms in addition to the overexpression of efflux pumps such as P-gp. Our earlier studies have clearly demonstrated that the activity of P-gp can sensitize MDR cells. The toxicity of MDR-

selective compounds such as **1a** is increased in a wide range of P-gp-expressing cells, and is abrogated by the downregulation or chemical inhibition of P-gp (Figure 3) [15,21,40,43]. Our results confirm that multidrug-resistant cells exhibit collateral sensitivity to selected compounds. However, in contrast to the isatin- $\beta$ -thiosemicarbazones (**1a-e**), the selective toxicity of the newly investigated compounds (**2c**, **3a**, **4c**, **4b**, **5b**, **5a**, **6a**, **6b**) was not influenced by the P-gp inhibitor Tariquidar (TQ), suggesting that the observed hypersensitivity of the MDR cells cannot be exclusively linked to the activity of P-gp, and should be rather explained by off-target effects linked to other specific resistance mechanisms or the genetic drift of the selected cells [39,71,72]. In a similar manner, enhanced toxicity of the *N*-(2-mercaptopropionyl)glycine tiopronin against a subset of (but not all investigated) MDR cell lines expressing P-gp was explained by the inhibition of glutathionperoxidase (GPx) [73,74]. Another example is the natural product Austocystin D, which possesses increased toxicity against some MDR cell lines as a result of increased activation by cytochrome P450 [75]. Increased sensitivity of MDR cells to the antimetabolite 2-deoxy-d-glucose, the electron transport chain inhibitors rotenone and antimycin A [71,76,77] as well as certain P-gp-substrates [72,78–80] were explained by the ATP depleting effect of the transporter. According to this model, increased glycolysis compensates for the higher energy demand created by the “futile cycling” of the transporter [79,81,82], but the oxidative stress associated with oxidative phosphorylation ultimately results in the selective apoptosis of MDR cells [83]. ROS have not only been implicated in the paradoxical sensitivity of resistant cells, but also in the mechanism of toxicity of chelators [8,12,13].

Since the mechanism of action and therefore the target of MDR selective compounds is not known, there is no clear understanding of their structure-activity relationships.

Some of the compounds shown in Figure 2 have been reported earlier to show activity in diverse biological settings. In fact, compound classes III (**3a-g**) and VI (**6a-f**) are formed by 2-

Hydroxy-phenylhydrazones, which are described as pan assay interference compounds (PAINs) [65,66]. In a wide range of target-based assays, covering ion channels, enzymes, and protein-protein-interactions, this substructure has been reported to be problematic due to its reactivity, spectroscopic properties and the ability to form metal complexes as well as aggregates [65,66]. Redox active compounds might interfere with proteins, and by inactivating the target often lead to false positive results in target-directed drug discovery projects [66]. However, the same reactive, photosensitive, and redox-active compounds may be particularly suited for therapeutic uses in the areas of oncology, microbiology, and parasitology [65]. Here we use a phenotypic drug discovery (PDD) strategy [84,85] where we have no a priori assumption of the availability or activity of a particular molecular target and/or signaling pathway. PAINs may be also problematic because of possible interferences with several applied assays. Here assay dependent artefacts were excluded by using two complementary viability assays (Figure S2). In many cases not only free ligands, but also their metal complexes possess biological activity: picolinylidene TSC derivatives or their metal complexes have been reported to possess antimalarial [68], modest antibacterial [86], modest (to no) antifungal [87,88], but promising antitumor activity [88–90]. Salicylidene TSCs form redox-active complexes with various metal ions, including Ru(II) [91,92] and Cu(II) [93–95]. The free ligands and their Ni(II) [96], Cu(II), Ru(II) and Zn(II) [92,94,95] complexes were reported to possess antibacterial and antifungal activity. N4-phenyl-salicylidene TSC (**3a**) has also been reported to show antitumor activity [95,97], GABA<sub>A</sub> receptor inhibition [98] and a very weak inhibition of RR [99]. Similarly, the acetaniline TSC (**2p**) forms Cu(II) complexes with moderate antibacterial and antifungal activity [46]. Similar to TSCs, benzothiazoles are also able to form biologically active metal complexes and find application as antibacterial and antifungal [45,46,100–102], as well as antitumor agents [45,49,50,54,103,104].

Compound **6g**, the non-chelating derivative of the salicylidene hydrazinobenzothiazole **6a** lacks toxic activity. The DTP database contains the activity patterns of standard anticancer drugs and tens of thousands of candidate anticancer agents [41,42]. In a subset of compounds identified by the substructure search in the DTP the putative donor atoms are occupied or incorporated in ring systems. These compounds lacked toxicity, corroborating the essential requirement of chelation. Interestingly, within this non-chelating subset, four compounds show an outstandingly high toxicity. Even though they contain the substructure motive by which they were identified, their structure is very different from the other compounds: They are derivatives of the marine natural product Trabectedin (ecteinascidin-743, Figure S12 D), which is currently undergoing clinical trials (phase III) in the USA, while it is approved for cancer treatment in Europe [105–107].

In the designed library we observed a superior activity of NNS (and NNN) chelators over ONS chelators. According to the principle of hard and soft acids and bases (HSAB), chelators with distinct donor atoms will show a binding preference for different metal ions, and stabilize different oxidation states of these ions [108,109]. The investigated TSCs and hydrazinobenzothiazoles share a sulfur atom as a soft electron donor and a hydrazinic nitrogen as a hard donor. In the picolinylidene derivatives, the third Lewis base is the borderline pyridine nitrogen donor, while in the salicylidene derivatives the third donor atom is a hard Lewis base [108–110]. Therefore the salicylidene compounds might prefer harder metals than the picolinylidene derivatives [110]. A study comparing the stability of several metal complexes formed by the N4 unsubstituted salicyl- and pyridyl-carbaldehyde TSCs supports this general trend [111]. The different chelators might not only influence the stability of complexes formed with diverse metal ions, but also their redox properties. For example, ONS donors prefer higher oxidation states of iron and copper as compared to NNS donors. The primary mechanism of action of hard donor atom containing chelators may involve the

depletion of iron ions (exploited in iron overload disease), while soft donor atom chelators are more capable of enhancing the production of ROS upon complexation with iron [112,113].

Our conclusions were drawn based on a set of investigated TSCs and related hydrazino-benzothiazoles, but a different behaviour is possible for unrelated compound classes. Hall *et al.* compared the anticancer potential of picolinylidene hydrazinobenzothiazole **5b** with the corresponding benzoxazolyl derivative on a panel of 17 cancer cell lines. Both compounds, as well as their benzimidazolyl derivative, showed general antitumor activity in the nanomolar concentration range [54]. Sensitivity towards the NNS (NNN) or NNO (NNN) donor chelators was comparable in general, differences were rather small [54]. Yet, it might be possible, that in both cases, similarly to the reported salicylidene and acetaniline benzothiazoles, the benzothiazole moiety binds to the metal ion with the nitrogen rather than the sulfur [46,100,102].

Interestingly, superior activity of NNS over ONS chelators was also evident in the toxicity patterns within the DTP database. The analogs identified by the substructure search demonstrate high diversity that is presumably associated with distinct mechanisms of toxicity. In addition to free ligands, also complexes formed with diverse metal ions and NNS or ONS chelators were identified by the search in the database (Figures 9 and S9). It is important to note that the toxicity of the complexes is also dependent on the nature of the metal ions that are incorporated into the structure. Despite the structural diversity and the presence of metals, we find that the chelating donor atom set is a strong determinant of toxicity, as in the diverse set the NNS donor chelators show an increased toxic activity over the ONS donor chelators. Preferential toxicity associated with the NNS signature is no longer observed when the ability to form complexes is lost, as seen in the case of compounds in which the donor atoms are either incorporated into ring systems or are otherwise occupied by substituents. Comparing the two investigated aniline derivatives **2p** and **5d** with their picolinylidene derivatives **2c** and

**5b**, we found that the latter show a greater toxic potential. This observation might be explained by a combination of steric and electronic reasons influencing the complexation of metal ions. Additionally, this result shows that donor atoms alone are not the sole determinants of toxicity. As a further moiety for the fine-tuning of biological activity, the imino carbon of the Schiff bases has been suggested since substitution at this position was reported to affect the toxicity of several Schiff base chelators [13,51,52]. A subset of NNS chelators became more toxic upon methylation at the imino carbon. One out of three MMPs from the NNN chelator pairs showed a similar behavior. Comparison of measured data of compounds with and without matched pairs suggested a beneficial effect of methylation in case of NNS donor chelators (Figures 5D). In contrast, toxicity was not influenced by imino carbon methylation for the investigated ONS donor chelators (Figure S10).

The same trends could be observed in a larger set of DTP compounds. By separating molecules with unsubstituted and methylated imino carbons in the analysis of the NNS and ONS compounds identified in the DTP database, we found no significant influence of imino carbon methylation on the activity of ONS donors, while there was a tendency of higher toxicity among NNS donors with imino carbon methylation (Figure S13). However, our data does not allow a general conclusion regarding the role of imino carbon methylation in toxicity.

#### 4. Conclusions

We synthesized a library around chelator scaffolds possessing variable activity against MDR cell lines. While some of the newly investigated compounds show enhanced toxicity in MDR cells, detailed analysis indicate that the library does contain *bona fide* MDR-selective compounds, whose toxicity would be directly enhanced by P-glycoprotein. We find that NNS

and NNN donor chelators show superior toxicity as compared to ONS derivatives regardless of the resistance status of the investigated cell lines.

## 5. Experimental Section

### 5.1. Materials and Methods

Chemicals used for synthesis were procured from Acros Organics (Geel, Belgium), Alfa Aesar (Karlsruhe, Germany), Sigma-Aldrich (Schnelldorf, Germany) or TCI (Eschborn, Germany) and used without further purification. Column chromatography was performed using Silica gel 60 (40-63  $\mu\text{m}$ , Merck, Darmstadt, Germany) as stationary phase.  $^1\text{H}$  NMR and  $^{13}\text{C}$  NMR spectra were obtained on a Bruker Advance 500 spectrometer or on a Varian INOVA 400 MHz spectrometer, respectively.  $\text{DMSO-}d_6$  or  $\text{CDCl}_3$  were used as solvents. Standard pulse programs were applied. Chemical shifts are expressed in ppm values using the residual solvent peaks as internal standards ( $\text{DMSO-}d_6$  2.50; 39.52 ppm or  $\text{CDCl}_3$  7.26; 77.16 ppm) [114]. Elemental analyses of the final products were performed on a Vario EL elemental analyser (Hanau, Germany). The values for carbon, nitrogen and hydrogen are given in percentage. Purity of compounds, of which the elemental analysis did not fit, were confirmed to be  $\geq 95\%$  by HPLC-MS using a Perkin Elmer Series 200 micro LC system consisting of binary pumps, autosampler and UV/vis detector. A Kinetex XB C18 column \*2.6  $\mu\text{m}$ , 150x4.6 mm, 100 A was used for separation the samples. Gradient elution was used with solvent A: 0.1% formic acid in water and B: 0.1% formic acid in acetonitrile. The flow rate was 600  $\mu\text{l}/\text{min}$  and 10  $\mu\text{l}$  of samples were injected. The UV chromatogram was recorded at 254 nm. Mass spectrometric measurements were carried out on an AB Sciex 3200Q Trap tandem mass spectrometer equipped with Turbo V ion source. The instrument was scanned in Q1 mode in the range of 50-600 Da.



Commercially available derivatives of interest were obtained from DTP (NSC291330 (**2b**), NSC670963 (**2d**), NSC289100, NSC668332 (**2h**), NSC668336 (**2i**), asinex (asx\_BAS\_00069712 (**6f**)), enamine (ena\_T0512-7089 (**2n**), ena\_T5848162 (**4g**), ena\_T6047476 (**6d**), ena\_T6242988 (**4h**)), IBS (ibs\_STOCK2S-70644 (**1e**), ibs\_STOCK3S-52757 (**6g**), ibs\_STOCK4S-04301 (**6e**)), Kemiome (kem\_KOME-0110497 (**2a**)), Maybridge (mbr\_JFD\_01295 (**4e**), mbr\_RDR\_00069 (**2l**)), Otava (ota\_7210500057 (**3a**)), Specs (spc\_AB-337/13036073 (**4d**), spc\_AN-329/40239015 (**3d**)), UkrOrg (uko\_PB-00249083 (**2o**), uko\_PB-01068874 (**2m**), uko\_PB-05694495 (**3g**), uko\_PB-05734828 (**3e**), uko\_PB-05735012 (**3f**), uko\_PB-06424414 (**4f**), uko\_PB-90126051 (**6c**)).

Tariquidar was a kind gift from Dr. Susan Bates (NCI).

## 5.2. Compound Synthesis

General method: The Schiff bases were obtained by adding an ethanolic solution of the hydrazinyl component to the solution of the keto component in equimolar amounts, refluxing the mixture in the presence of catalytic amounts of acid. If not indicated otherwise, purification was carried out by recrystallization. Carbazides were prepared by adding an equimolar amount of hydrazine to the methanolic solution of the respective isothiocyanate [53]. For the picolinylidene derivatives with ethyl group in 5-position of the pyridine moiety (**2e**, **2k**), 5-Ethylpicolinaldehyde was prepared from 5-ethyl-2-methyl-pyridine as reported previously [13,115].  $^1\text{H}$  NMR (500 MHz,  $\text{CDCl}_3$ ):  $\delta$  = 10.03 (s, 1H), 8.60 (d, 1H,  $^4J(\text{H,H})$  = 1.9 Hz), 7.87 (d, 1H,  $^3J(\text{H,H})$  = 8.0 Hz), 7.70 – 7.63 (m, 1H), 2.73 (q, 2H,  $^3J(\text{H,H})$  = 7.6 Hz), 1.28 (t, 3H,  $^3J(\text{H,H})$  = 7.6 Hz).  $^{13}\text{C}$  NMR (500 MHz,  $\text{CDCl}_3$ ):  $\delta$  = 193.3, 151.1, 150.2, 144.7, 136.3, 121.7, 26.4, 15.0.

### 5.2.1. Preparation of Carbazides:

**5.2.1.1. *N*-(4-methoxyphenyl)hydrazinecarbothioamide (C-1)**

The reaction of 4-methoxyphenylisothiocyanate (1.000 g, 6.052 mmol) with hydrazine (0.37 mL 80% aqueous, 6.052 mmol) resulted in white crystals of the product in 97.4% yield (1.163 g, 5.90 mmol). <sup>1</sup>H-NMR (500 MHz, DMSO-*d*<sub>6</sub>): δ = 9.51 (s, 1H), 8.94 (s, 1H), 7.44 (d, 2H, <sup>3</sup>*J*(H,H) = 8.2 Hz), 6.88 – 6.83 (m, 2H), 4.70 (s, 2H), 3.74 (s, 3H). <sup>13</sup>C-NMR (126 MHz, DMSO-*d*<sub>6</sub>): δ = 179.8, 156.1, 132.2, 125.5, 113.2, 55.2.

**5.2.1.2. *N*-(4-tolyl)hydrazinecarbothioamide (C-2)**

The reaction of 4-tolylisothiocyanate (500 mg, 3.35 mmol) with hydrazine (0.20 mL 80% aqueous, 3.35 mmol) resulted in white needles of the product in 97.8% yield (594 mg, 3.27 mmol). <sup>1</sup>H-NMR (500 MHz, DMSO-*d*<sub>6</sub>): δ = 9.55 (s, 1H), 9.00 (s, 1H), 7.49 (d, 2H, <sup>3</sup>*J*(H,H) = 7.2 Hz), 7.10 (d, 2H, <sup>3</sup>*J*(H,H) = 8.2 Hz), 4.74 (s, 2H), 2.27 (s, 3H). <sup>13</sup>C-NMR (126 MHz, DMSO-*d*<sub>6</sub>): δ = 179.5, 136.6, 133.1, 128.5 (2C), 123.5 (2C), 20.4.

**5.2.2.3. *N*-(4-nitrophenyl)hydrazinecarbothioamide (C-3)**

The reaction of 4-nitrophenylisothiocyanate (1.000 g, 5.56 mmol) with hydrazine (0.34 mL 80% aqueous, 5.56 mmol), was carried out in a mixture of toluene and methanol, due to the low solubility of the starting material and resulted in ochre product crystals in 92.8% yield (1.095 g, 5.16 mmol). <sup>1</sup>H-NMR (500 MHz, DMSO-*d*<sub>6</sub>): δ = 9.55 (s, 1H), 8.14 (s, 4H), 7.83 (s, 1H), 6.55 (bs, 2H). <sup>13</sup>C-NMR (126 MHz, DMSO-*d*<sub>6</sub>): δ = 178.8, 145.7, 142.5, 123.8 (2C), 122.0 (2C).

**5.2.3. Preparation of isatin-β-thiosemicarbazones (Figures 1, 2, box I):****5.2.3.1. *N*-(4'-methoxyphenyl)-2-(2-oxoindoline-3-ylidene)hydrazinecarbothioamide (1a)**

The reaction of isatin (147.13 mg, 1.0 mmol) with *N*-(4-methoxyphenyl)hydrazinecarbothioamide **C-1** (197.26 mg, 1.0 mmol) in ethanolic solution under HCl-catalysis resulted in a yellow fluffy precipitate, which was identified as the product in 89 % yield (291 mg, 0.89 mmol). <sup>1</sup>H-NMR (500 MHz, DMSO-*d*<sub>6</sub>): δ = 12.75 (s, 1H), 11.22 (s, 1H), 10.70 (s, 1H), 7.76 (d, 1H, <sup>3</sup>*J*(H,H) = 7.6 Hz), 7.50 – 7.44 (m, 2H), 7.36 (td, 1H, <sup>3</sup>*J*(H,H) = 7.7 Hz, <sup>4</sup>*J*(H,H) = 1.3 Hz), 7.13 – 7.08 (m, 1H), 6.99 – 6.95 (m, 2H), 6.94 (d, 1H, <sup>3</sup>*J*(H,H) = 7.9 Hz), 3.78 (s, 3H). <sup>13</sup>C-NMR (126 MHz, DMSO-*d*<sub>6</sub>): δ = 176.5, 162.6, 157.4, 142.4, 132.0, 131.28, 131.25, 127.1, 122.3, 121.3 (2C), 119.9, 113.5 (2C), 111.0, 55.3. Anal. Calcd. for C<sub>16</sub>H<sub>14</sub>N<sub>4</sub>SO<sub>2</sub>: C: 58.88; H: 4.32; N: 17.17. Found: C: 58.58; H: 4.349; N: 16.95.

#### 5.2.3.2. *N*-(4'-methoxyphenyl)-2-(2-oxo-5-(trifluoromethoxy)-indoline-3-ylidene)-hydrazinecarbothioamide (**1b**)

The reaction of 5-trifluoromethoxyisatin (50 mg, 0.22 mmol) with *N*-(4-methoxyphenyl)hydrazinecarbothioamide **C-1** (43 mg, 0.22 mmol) in ethanolic solution under HCl-catalysis resulted in a yellow fluffy precipitate, which was identified as the product in 70 % yield (65.7 mg, 0.16 mmol). <sup>1</sup>H-NMR (500 MHz, DMSO-*d*<sub>6</sub>): δ = 12.60 (s, 1H), 11.36 (s, 1H), 10.78 (s, 1H), 7.78 (s, 1H), 7.49 – 7.41 (m, 2H), 7.41 – 7.31 (m, 1H), 7.02 (d, 1H, <sup>3</sup>*J*(H,H) = 5.0 Hz), 7.01 – 6.95 (m, 2H), 3.78 (s, 3H). <sup>13</sup>C-NMR (126 MHz, DMSO-*d*<sub>6</sub>): δ = 176.6, 162.7, 157.5, 143.5, 141.2, 131.1, 130.9, 127.3 (2C), 124.0, 121.5, 120.7 (d {121.19, 119.15}), <sup>1</sup>*J*(C,F) = 255.7 Hz, 114.4 (2C), 113.6, 112.1, 55.3. Anal. Calcd. for C<sub>17</sub>H<sub>13</sub>N<sub>4</sub>SO<sub>3</sub>F<sub>3</sub>: C: 49.76; H: 3.19; N: 13.65. Found: C: 49.61; H: 3.477; N: 13.53.

#### 5.2.3.3. *N*-(4'-tolyl)-2-(2-oxoindoline-3-ylidene)hydrazinecarbothioamide (**1c**) [44]

The reaction of isatin (147.13 mg, 1.0 mmol) with *N*-(4-tolyl)hydrazinecarbothioamide **C-2** (181.26 mg, 1.0 mmol) in ethanolic solution under acetic acid catalysis resulted in a yellow

fluffy precipitate, which was identified as the product in 53 % yield (162.8 mg, 0.53 mmol). <sup>1</sup>H-NMR (500 MHz, DMSO-*d*<sub>6</sub>): δ = 12.78 (s, 1H), 11.22 (s, 1H), 10.71 (s, 1H), 7.78 (d, 1H, <sup>3</sup>*J*(H,H) = 7.5 Hz), 7.49 (d, 2H, <sup>3</sup>*J*(H,H) = 8.3 Hz), 7.36 (td, 1H, <sup>4</sup>*J*(H,H) = 1.2 Hz, <sup>3</sup>*J*(H,H) = 7.7 Hz), 7.22 (d, 2H, <sup>3</sup>*J*(H,H) = 8.2 Hz), 7.10 (td, 1H, <sup>4</sup>*J*(H,H) = 0.7 Hz, <sup>3</sup>*J*(H,H) = 7.6 Hz), 6.94 (d, 1H, <sup>3</sup>*J*(H,H) = 7.8 Hz), 2.33 (s, 3H). <sup>13</sup>C-NMR (126 MHz, DMSO-*d*<sub>6</sub>): δ = 176.3, 162.6, 142.4, 135.9, 135.3, 132.1, 131.3, 128.8 (2C), 125.4 (2C), 122.3, 121.3, 119.9, 111.0, 20.6. Anal. Calcd. for C<sub>16</sub>H<sub>14</sub>N<sub>4</sub>SO: C: 61.92; H: 4.55; N: 18.05. Found: C: 62.4; H: 4.402; N: 18.54.

**5.2.3.4. *N*-(4'-nitrophenyl)-2-(2-oxoindoline-3-ylidene)hydrazinecarbothioamide (1d)**  
[44]

The reaction of isatin (147.13 mg, 1.0 mmol) with *N*-(4-tolyl)hydrazinecarbothioamide **C-3** (212.23 mg, 1.0 mmol) in ethanolic solution under acetic acid catalysis resulted in an orange-yellowish fluffy precipitate, which was identified as the product in 71 % yield (242 mg, 0.71 mmol). <sup>1</sup>H-NMR (500 MHz, DMSO-*d*<sub>6</sub>): δ = 13.01 (s, 1H), 11.28 (s, 1H), 11.10 (s, 1H), 8.36 – 8.24 (m, 2H), 8.14 – 8.03 (m, 2H), 7.78 (d, 1H, <sup>3</sup>*J*(H,H) = 7.4 Hz), 7.40 (td, 1H, <sup>4</sup>*J*(H,H) = 1.2 Hz, <sup>3</sup>*J*(H,H) = 7.7 Hz), 7.13 (td, 1H, <sup>4</sup>*J*(H,H) = 0.8 Hz, <sup>3</sup>*J*(H,H) = 7.6 Hz), 6.96 (d, 1H, <sup>3</sup>*J*(H,H) = 7.8 Hz). <sup>13</sup>C-NMR (126 MHz, DMSO-*d*<sub>6</sub>): δ = 176.0, 162.7, 144.6, 144.1, 142.7, 133.27, 131.8, 124.6 (2C), 123.9 (2C), 122.4, 121.5, 119.6, 111.2. Anal. Calcd. for C<sub>15</sub>H<sub>11</sub>N<sub>5</sub>SO<sub>3</sub>: C: 52.78; H: 3.25; N: 20.52. Found: C: 53.24; H: 3.57; N: 20.9.

**5.2.4. Preparation of picolinylidene thiosemicarbazones** (Figures 1, 2, box II):

**5.2.4.1. *N*-(4'-methoxyphenyl)-2-(1-(pyridin-2-yl)ethylidene)hydrazinecarbothioamide (2c)**

The reaction of 1-(pyridin-2-yl)ethanone (0.15 mL, 1.325 mmol) with *N*-(4-tolyl)hydrazinecarbothioamide **C-2** (250 mg, 1.325 mmol) in ethanolic solution under acetic acid catalysis resulted in a white precipitate, which was recrystallized to afford the product in 62.9 % yield (250.6 mg, 0.83 mmol). <sup>1</sup>H-NMR (500 MHz, DMSO-*d*<sub>6</sub>): δ = 10.54 (s, 1H), 10.07 (s, 1H), 8.60 (ddd, 1H, <sup>5</sup>*J*(H,H) = 0.9 Hz, <sup>4</sup>*J*(H,H) = 1.9 Hz, <sup>3</sup>*J*(H,H) = 4.7 Hz), 8.54 (d, 1H, <sup>3</sup>*J*(H,H) = 8.2 Hz), 7.84 – 7.75 (sm, 1H), 7.43 – 7.36 (sm, 3H), 6.97 – 6.91 (sm, 2H), 3.78 (s, 3H), 2.46 (s, 3H). <sup>13</sup>C-NMR (126 MHz, DMSO-*d*<sub>6</sub>): δ = 177.7, 157.2, 154.7, 49.0, 148.6, 136.5, 132.2, 127.9 (2C), 124.2, 121.3, 113.5 (2C), 55.4, 12.50. Anal. Calcd. for C<sub>15</sub>H<sub>16</sub>N<sub>4</sub>SO: C: 59.98; H: 5.37; N: 18.65. Found: C: 60.0; H: 5.3; N: 18.76.

#### 5.2.4.2. **2-((5-ethylpyridin-2-yl)methylene)-*N*-(4'-methoxyphenyl)hydrazinecarbothioamide (2e)**

The reaction of 5-ethylpicolinaldehyde (200 mg, 1.48 mmol) with *N*-(4-methoxyphenyl)hydrazinecarbothioamide **C-1** (291.9 mg, 1.48 mmol) in ethanolic solution under acetic acid catalysis resulted in white crystals, of product in 60 % yield (229 mg, 0.73 mmol). The product seemed to be thermo labile, since it decomposed upon a further recrystallization trial. <sup>1</sup>H-NMR (500 MHz, DMSO-*d*<sub>6</sub>): δ = 11.87 (s, 1H), 10.09 (s, 1H), 8.44 (dd, 1H, <sup>5</sup>*J*(H,H) = 0.5 Hz, <sup>4</sup>*J*(H,H) = 1.9 Hz), 8.35 (d, 1H, <sup>3</sup>*J*(H,H) = 8.2 Hz), 8.17 (s, 1H), 7.69 (dd, 1H, <sup>4</sup>*J*(H,H) = 2.2 Hz, <sup>3</sup>*J*(H,H) = 8.2 Hz), 7.43 – 7.37 (sm, 2H), 6.97 – 6.91 (sm, 2H), 3.77 (s, 3H), 2.65 (q, 2H, <sup>3</sup>*J*(H,H) = 7.6 Hz), 1.21 (t, 3H, <sup>3</sup>*J*(H,H) = 7.6 Hz). <sup>13</sup>C-NMR (126 MHz, DMSO-*d*<sub>6</sub>): δ = 176.6, 157.0, 150.9, 148.7, 142.9, 139.8, 135.7, 131.8, 127.6 (2C), 120.2, 113.3 (2C), 55.2, 25.2, 15.1. Purity was determined with HPLC-MS to be ≥ 95% (m/z calculated for [M]: 314.41, found 315.2 for [M + H]<sup>+</sup>).

#### 5.2.4.3. **2-(pyridin-2-ylmethylene)-*N*-(4'-tolyl)hydrazinecarbothioamide (2f)**

The reaction of pyridine-2-carbaldehyde (160.7 mg, 1.5 mmol) with *N*-(4-tolyl)hydrazinecarbothioamide **C-2** (271.9 mg, 1.5 mmol) in ethanolic solution under acetic acid catalysis resulted in a white fluffy precipitate, which was identified as the product in 82.5 % yield (334.5 mg, 1.237 mmol). <sup>1</sup>H-NMR (500 MHz, DMSO-*d*<sub>6</sub>): δ = 11.95 (s, 1H), 10.15 (s, 1H), 8.58 (ddd, 1H, <sup>5</sup>*J*(H,H) = 1.0 Hz, <sup>4</sup>*J*(H,H) = 1.7 Hz, <sup>3</sup>*J*(H,H) = 4.9 Hz), 8.43 (d, 1H, <sup>3</sup>*J*(H,H) = 8.0 Hz), 8.19 (s, 1H), 7.84 (ddd, 1H, <sup>5</sup>*J*(H,H) = 0.9 Hz, <sup>4</sup>*J*(H,H) = 1.8 Hz, <sup>3</sup>*J*(H,H) = 7.6 Hz), 7.44 – 7.40 (m, 2H), 7.39 (ddd, 1H, <sup>3</sup>*J*(H,H) = 1.2 Hz, <sup>3</sup>*J*(H,H) = 4.9 Hz, <sup>3</sup>*J*(H,H) = 7.5 Hz), 7.18 (d, 2H, <sup>3</sup>*J*(H,H) = 8.0 Hz), 2.32 (s, 3H). <sup>13</sup>C-NMR (126 MHz, DMSO-*d*<sub>6</sub>): δ = 176.5, 153.3, 149.4, 143.0, 136.5, 136.5, 134.7, 128.6 (2C), 126.0 (2C), 124.2, 120.6, 20.7. Anal. Calcd. for C<sub>14</sub>H<sub>14</sub>N<sub>4</sub>S: C: 62.2; H: 5.22; N: 20.72. Found: C: 62.36; H: 5.228; N: 20.93.

#### 5.2.4.4. 2-(1-(pyridin-2-yl)ethylidene)-*N*-(4'-tolyl)hydrazinecarbothioamide (2g)

The reaction of 1-(pyridin-2-yl)ethanone (0.17 mL, 1.5 mmol) with *N*-(4-tolyl)hydrazinecarbothioamide **C-2** (271.9 mg, 1.5 mmol) in ethanolic solution under acetic acid catalysis resulted in white crystals, which were recrystallized from a CHCl<sub>3</sub>:EtOH mixture (1.5:1) to afford the product in 40.8 % yield (174 mg, 0.61 mmol). <sup>1</sup>H-NMR (500 MHz, DMSO-*d*<sub>6</sub>): δ = 10.58 (s, 1H), 10.10 (s, 1H), 8.60 (ddd, 1H, <sup>5</sup>*J*(H,H) = 0.9 Hz, <sup>4</sup>*J*(H,H) = 1.7, <sup>3</sup>*J*(H,H) = 4.7 Hz), 8.52 (d, 1H, <sup>3</sup>*J*(H,H) = 8.2 Hz), 7.81 (ddd, 1H, <sup>5</sup>*J*(H,H) = 1.9 Hz, <sup>5</sup>*J*(H,H) = 7.4 Hz, <sup>5</sup>*J*(H,H) = 8.2 Hz), 7.45 – 7.37 (m, 3H), 7.18 (d, 2H, <sup>3</sup>*J*(H,H) = 7.9 Hz), 2.46 (s, 3H), 2.32 (s, 3H). <sup>13</sup>C-NMR (126 MHz, DMSO-*d*<sub>6</sub>): δ = 177.3, 154.5, 149.0, 148.4, 136.5, 136.3, 134.7, 128.5 (2C), 125.9 (2C), 124.0, 121.2, 20.6, 12.4. Anal. Calcd. for C<sub>15</sub>H<sub>16</sub>N<sub>4</sub>S: C: 63.35; H: 5.67; N: 19.70. Found: C: 62.92; H: 5.602; N: 19.81.

#### 5.2.4.5. 2-(pyridin-2-ylmethylene)-*N*-(4-nitrophenyl)hydrazinecarbothioamide (2j)

The reaction of picolin aldehyde (160.7 mg, 1.5 mmol) with *N*-(4-nitrophenyl)hydrazinecarbothioamide **C-3** (318.3 mg, 1.5 mmol) in ethanolic solution under acetic acid catalysis resulted in a bright yellow fluffy precipitate, which was recrystallized to afford the product in 97 % yield (437 mg, 1.45 mmol). <sup>1</sup>H-NMR (500 MHz, DMSO-*d*<sub>6</sub>): δ = 12.34 (s, 1H), 10.53 (s, 1H), 8.61 (ddd, 1H, <sup>5</sup>*J*(H,H) = 0.9 Hz, <sup>4</sup>*J*(H,H) = 1.6 Hz, <sup>3</sup>*J*(H,H) = 4.8 Hz), 8.41 (d, 1H, <sup>3</sup>*J*(H,H) = 8.0 Hz), 8.28 – 8.23 (m, 3H), 8.08 – 8.03 (m, 2H), 7.89 (td, 1H, <sup>4</sup>*J*(H,H) = 1.5 Hz, <sup>3</sup>*J*(H,H) = 7.7 Hz), 7.43 (ddd, 1H, <sup>5</sup>*J*(H,H) = 1.1 Hz, <sup>4</sup>*J*(H,H) = 4.9 Hz, <sup>3</sup>*J*(H,H) = 7.5 Hz). <sup>13</sup>C-NMR (126 MHz, DMSO-*d*<sub>6</sub>): δ = 175.8, 152.8, 149.4, 145.2, 144.2, 143.6, 136.5, 124.7 (2C), 124.5, 123.7 (2C), 120.7. Anal. Calcd. for C<sub>13</sub>H<sub>11</sub>N<sub>5</sub>SO<sub>2</sub>: C: 51.82; H: 3.68; N: 23.24. Found: C: 52.13; H: 3.679; N: 23.51.

#### 5.2.4.6. 2-((5-ethylpyridin-2-yl)methylene)-*N*-(4'-nitrophenyl)hydrazinecarbothioamide (**2k**)

The reaction of 5-ethylpicolin aldehyde (202.74 mg, 1.5 mmol) with *N*-(4-nitrophenyl)hydrazinecarbothioamide **C-3** (318.3 mg, 1.5 mmol) in ethanolic solution under acetic acid catalysis resulted in orange crystals, which delivered the pure product in 49 % yield (242 mg, 0.74 mmol) after column chromatography and recrystallization. <sup>1</sup>H-NMR (500 MHz, DMSO-*d*<sub>6</sub>): δ = 12.21 (bs, 1H), 10.52 (bs, 1H), 8.47 (d, 1H, <sup>4</sup>*J*(H,H) = 1.6 Hz), 8.32 (d, 1H, <sup>3</sup>*J*(H,H) = 7.9 Hz), 8.27 – 8.24 (sm, 2H), 8.23 (s, 1H), 8.07 – 8.03 (sm, 2H), 7.74 (dd, 1H, <sup>4</sup>*J*(H,H) = 2.0 Hz, <sup>3</sup>*J*(H,H) = 8.4 Hz), 2.67 (q, 2H, <sup>3</sup>*J*(H,H) = 7.6 Hz), 1.22 (t, 3H, <sup>3</sup>*J*(H,H) = 7.6 Hz). <sup>13</sup>C-NMR (126 MHz, DMSO-*d*<sub>6</sub>): δ = 175.7, 150.5, 148.9, 145.3, 144.4, 143.5, 140.2, 135.8, 124.6, 123.7 (2C), 120.4 (2C), 25.3, 15.1. Anal. Calcd. for C<sub>15</sub>H<sub>15</sub>N<sub>5</sub>SO<sub>2</sub>×0.5 H<sub>2</sub>O: C: 53.24; H: 4.77; N: 20.70. Found: C: 53.44; H: 4.72; N: 20.75.

### 5.2.5. Preparation of the acetanilide thiosemicarbazone (1-(1-(2-aminophenyl)-ethylidene)amino)-3-(4'-methoxyphenyl)thiourea (2p)

The reaction of 2-aceto-aniline (0.11 mL, 1.27 mmol) with 2-hydrazinobenzothiazole (250 mg, 1.27 mmol) in ethanolic solution under acetic acid catalysis delivered the product as a bright yellow solid in < 9.5 % yield (38 mg, 0.121 mmol) after column chromatography (PE:EE 4:1) and recrystallization. <sup>1</sup>H-NMR (500 MHz, DMSO-*d*<sub>6</sub>): δ = 10.44 (s, 1H), 9.69 (s, 1H), 7.46 (d, 2H, <sup>3</sup>*J*(H,H) = 9.1 Hz), 7.36 (dd, 1H, <sup>4</sup>*J*(H,H) = 1.4 Hz, <sup>3</sup>*J*(H,H) = 8.0 Hz), 7.06 – 7.01 (sm, 1H), 6.92 – 6.88 (m, 2H), 6.71 (dd, 1H, <sup>4</sup>*J*(H,H) = 1.1 Hz, <sup>3</sup>*J*(H,H) = 8.0 Hz), 6.57 – 6.52 (sm, 1H), 3.75 (s, 3H), 2.32 (s, 3H) – NH<sub>2</sub> not visible. The purity of this compound was estimated with HPLC-MS method to be between 75 and 85% (m/z calculated for [M]: 314.41, found 315.2 for [M + H]<sup>+</sup>).

### 5.2.6. Preparation of salicylidene thiosemicarbazones (Figures 1, 2, box III):

#### 5.2.6.1. 2-(2-hydroxybenzylidene)-*N*-(4'-methoxyphenyl)hydrazinecarbothioamide (3b)

Salicylic aldehyde (0.135 mL, 1.267 mmol) was reacted with *N*-(4-methoxyphenyl)hydrazinecarbothioamide **C-1** (250 mg, 1.267 mmol) in ethanolic solution under acetic acid catalysis. The crude product was purified with column chromatography (PE:EE 4:1) and allowed to crystallize at -20°C. The product was obtained as white crystals in a yield of 61.8 % (236 mg, 0.78 mmol). <sup>1</sup>H-NMR (500 MHz, CDCl<sub>3</sub>): δ = 10.92 (s, 1H), 8.55 (s, 1H), 7.52 – 7.48 (sm, 2H), 7.37 – 7.31 (m, 2H), 7.29 (dd, 1H, <sup>4</sup>*J*(H,H) = 1.6 Hz, <sup>3</sup>*J*(H,H) = 7.6 Hz), 7.04 (d, 1H, <sup>3</sup>*J*(H,H) = 7.9 Hz), 6.95 (td, 1H, <sup>4</sup>*J*(H,H) = 1.1 Hz, <sup>3</sup>*J*(H,H) = 7.6 Hz), 6.89 – 6.84 (sm, 2H), 3.79 (s, 3H) – OH not visible. <sup>13</sup>C-NMR (126 MHz, CDCl<sub>3</sub>): δ = 158.9, 158.8, 156.8, 150.0, 132.2, 131.8, 131.5, 122.4 (2C), 119.8, 118.3, 117.0, 114.4 (2C), 55.7. Anal. Calcd. for C<sub>15</sub>H<sub>15</sub>N<sub>3</sub>SO<sub>2</sub>: C: 59.78; H: 5.02; N: 13.94. Found: C: 59.75; H: 5.047; N: 14.11.



### 5.2.6.2. 2-(2-hydroxybenzylidene)-*N*-(4'-tolyl)hydrazinecarbothioamide (3c)

The reaction of salicylic aldehyde (0.147 mL, 1.379 mmol) with *N*-(4-tolyl)hydrazinecarbothioamide **C-2** (250 mg, 1.267 mmol) in ethanolic solution under acetic acid catalysis resulted in yellowish crystals, which delivered the pure product in 34 % yield (133.8 mg, 0.47 mmol) after recrystallization. <sup>1</sup>H-NMR (500 MHz, DMSO-*d*<sub>6</sub>): δ = 11.67 (s, 1H), 9.94 (s, 1H), 8.48 (s, 1H), 8.04 (d, 1H, <sup>3</sup>*J*(H,H) = 7.6 Hz), 7.45 – 7.39 (sm, 2H), 7.25 – 7.20 (sm, 1H), 7.15 (d, 2H, <sup>3</sup>*J*(H,H) = 8.1 Hz), 6.87 (dd, 1H, <sup>4</sup>*J*(H,H) = 0.9 Hz, <sup>3</sup>*J*(H,H) = 8.2 Hz), 6.82 (t, 1H, <sup>3</sup>*J*(H,H) = 7.5 Hz), 2.30 (s, 3H). <sup>13</sup>C NMR (101 MHz, DMSO-*d*<sub>6</sub>): δ = 175.8, 156.5, 139.9, 136.6, 134.3, 131.2, 128.5 (2C), 127.1, 125.6 (2C), 120.3, 119.2, 116.04, 20.6. Anal. Calcd. for C<sub>15</sub>H<sub>15</sub>N<sub>3</sub>SO: C: 63.13; H: 5.30; N: 14.73. Found: C: 63.12; H: 5.249; N: 14.89.

### 5.2.7. Preparation of picolinylidene hydrazinobenzothiazoles (Figures 1, 2, box V):

As a general comment on the hydrazinobenzothiazole derivatives from boxes V, VI and VII, in the <sup>13</sup>C NMR spectra (especially measured by attached proton test (APT) method) some signals were not detectable. Mainly this occurred for the bridging quaternary carbons *C-3'a* and *C-7'a*, but dependent on the respective compounds also for some other signals. Those are indicated below.

#### 5.2.7.1. 2'-(2-(pyridin-2-yl)methylene)hydrazinyl)-1',3'-benzothiazole (5a)

The reaction of picolinaldehyde (0.144 mL, 1.513 mmol) with 2-hydrazinobenzothiazole (250 mg, 1.513 mmol) in ethanolic solution under acetic acid catalysis resulted in bright yellowish shining crystals, which delivered the pure product in 74.8 % yield (287.7 mg, 1.132 mmol) after recrystallization. <sup>1</sup>H-NMR (500 MHz, DMSO-*d*<sub>6</sub>): δ = 12.48 (bs, 1H), 8.60 (ddd, 1H, <sup>5</sup>*J*(H,H) = 1.0 Hz, <sup>4</sup>*J*(H,H) = 1.7 Hz, <sup>3</sup>*J*(H,H) = 5.0 Hz), 8.14 (s, 1H), 7.91 (d, 1H,

$^3J(\text{H,H}) = 7.9$  Hz), 7.87 (m, 1H), 7.80 (d, 1H,  $^3J(\text{H,H}) = 7.9$  Hz), 7.49 (d, 1H,  $^3J(\text{H,H}) = 5.9$  Hz), 7.38 (ddd, 1H,  $^4J(\text{H,H}) = 1.6$  Hz,  $^3J(\text{H,H}) = 4.9$  Hz,  $^3J(\text{H,H}) = 7.3$  Hz), 7.35 – 7.29 (sm, 1H), 7.17 – 7.10 (sm, 1H).  $^{13}\text{C-NMR}$  (101 MHz,  $\text{DMSO-}d_6$ ):  $\delta = 167.1, 153.1, 149.5, 136.8, 126.0, 123.9, 121.9, 121.6, 119.4$ . Signals for  $\text{HC=N}$ ,  $C-3$ ,  $C-3'a$  and  $C-7'a$  were not detectable. Anal. Calcd. for  $\text{C}_{13}\text{H}_{10}\text{N}_4\text{S}$ : C: 61.4; H: 3.96; N: 22.03. Found: C: 61.81; H: 3.936; N: 22.4. Purity was additionally determined with HPLC-MS to be  $\geq 95\%$  (m/z calculated for  $[\text{M}]$ : 254.31, found 255.2 for  $[\text{M} + \text{H}]^+$ ).

#### 5.2.7.2. 2'-(2-(1-(pyridin-2-yl)ethylidene)hydrazinyl)-1',3'-benzothiazole (5b)

The reaction of 1-(pyridin-2-yl)ethanone (0.17 mL, 1.513 mmol) with 2-hydrazinobenzothiazole (250 mg, 1.513 mmol) in ethanolic solution under acetic acid catalysis resulted in beige precipitate, which delivered the pure product after recrystallization. The yield was not determined. NMRs revealed the presence of acetic acid in the crystals, therefore EA analysis was adapted accordingly.  $^1\text{H-NMR}$  (500 MHz,  $\text{DMSO-}d_6$ ):  $\delta = 11.86$  (bs, 1H), 8.59 (ddd, 1H,  $^5J(\text{H,H}) = 0.9$  Hz,  $^4J(\text{H,H}) = 1.6$  Hz,  $^3J(\text{H,H}) = 4.7$  Hz), 8.08 (d, 1H,  $^3J(\text{H,H}) = 8.2$  Hz), 7.90 – 7.83 (sm, 1H), 7.74 (d, 1H,  $^3J(\text{H,H}) = 7.6$  Hz), 7.41 – 7.36 (sm, 2H), 7.33 – 7.27 (sm, 1H), 7.11 (td, 1H,  $^4J(\text{H,H}) = 0.9$  Hz,  $^3J(\text{H,H}) = 7.8$  Hz), 2.43 (s, 3H).  $^{13}\text{C-NMR}$  (126 MHz,  $\text{DMSO-}d_6$ ):  $\delta = 168.2, 155.1, 148.6, 136.4, 126.0, 123.5, 121.7, 121.7, 119.7, 12.7$  – the signals for  $\text{CH}_3\text{C=N}$ ,  $C-3$ ,  $C-3'a$ ,  $C-7'a$  were not detectable. Anal. Calcd. for  $\text{C}_{14}\text{H}_{12}\text{N}_4\text{S} \times 0.7 \text{ C}_2\text{H}_4\text{O}_2$ : C: 59.6; H: 4.8; N: 18.1. Found: C: 59.1; H: 4.9; N: 18.0. Additionally purity was determined with HPLC-MS to be  $\geq 95\%$  (m/z calculated for  $[\text{M}]$ : 268.34, found 268.8 for  $[\text{M} + \text{H}]^+$ , 291.3 for  $[\text{M} + \text{Na}]^+$ ).

#### 5.2.7.3. 2'-(2-(5-ethylpyridin-2-yl)methylene)hydrazinyl)-1',3'-benzothiazole (5c)

The reaction of 5-ethyl-picolinaldehyde (200 mg, 1.48 mmol) with 2-hydrazinobenzothiazole (244.5 mg, 1.480 mmol) in ethanolic solution under acetic acid catalysis resulted in cream-colored precipitate, which delivered the pure product in 46 % yield (192.2 mg, 0.681 mmol) after recrystallization.  $^1\text{H-NMR}$  (500 MHz,  $\text{DMSO-}d_6$ ):  $\delta$  = 12.41 (bs, 1H), 8.46 (dd, 1H,  $^5J(\text{H,H}) = 0.6$  Hz,  $^4J(\text{H,H}) = 2.1$  Hz), 8.13 (s, 1H), 7.84 (d, 1H,  $^3J(\text{H,H}) = 7.9$  Hz), 7.79 (d, 1H,  $^3J(\text{H,H}) = 7.9$  Hz), 7.73 (ddd, 1H,  $^3J(\text{H,H}) = 0.5$  Hz,  $^3J(\text{H,H}) = 2.1$  Hz,  $^3J(\text{H,H}) = 8.2$  Hz), 7.48 (d, H,  $^3J(\text{H,H}) = 4.8$  Hz), 7.31 (td, 1H,  $^3J(\text{H,H}) = 1.3$  Hz,  $^3J(\text{H,H}) = 8.0$  Hz), 7.17 – 7.10 (sm, 1H), 2.66 (q, 2H,  $^3J(\text{H,H}) = 7.7$  Hz), 1.21 (t, 3H,  $^3J(\text{H,H}) = 7.7$  Hz).  $^{13}\text{C-NMR}$  (126 MHz,  $\text{DMSO-}d_6$ ): 167.0, 150.8, 148.9, 139.4, 136.0, 126.0, 121.8, 121.5, 119.0, 25.2, 15.1 – the signals for HC=N, C-3, C-3'a, C-7'a were not visible. Anal. Calcd. for  $\text{C}_{15}\text{H}_{14}\text{N}_4\text{S}$ : C: 63.80; H: 5.00; N: 19.84. Found: C: 63.47; H: 4.886; N: 19.81.

#### 5.2.8. Preparation of the acetaniline hydrazinobenzothiazole 2-(1-(2-(1',3'-benzothiazol-2'-yl)hydrazine-1-ylidene)ethyl)aniline (5d):

The reaction of 2-aceto-aniline (0.10 mL, 1.21 mmol) with 2-hydrazinobenzothiazole (200 mg, 1.21 mmol) in ethanolic solution under acetic acid catalysis delivered the product as a greyish brownish solid after recrystallization.

$^1\text{H-NMR}$  (500 MHz,  $\text{DMSO-}d_6$ ):  $\delta$  = 11.62 (s, 1H), 7.67 (d, 1H,  $^3J(\text{H,H}) = 7.9$  Hz), 7.43 (dd, 1H,  $^4J(\text{H,H}) = 1.4$  Hz,  $^3J(\text{H,H}) = 8.0$  Hz), 7.30 – 7.19 (m, 2H), 7.10 – 7.00 (m, 2H), 6.82 (s, 2H), 6.76 (dd, 1H,  $^4J(\text{H,H}) = 1.3$  Hz,  $^3J(\text{H,H}) = 8.2$  Hz), 6.61 – 6.51 (sm, 1H), 2.43 (s, 3H).  $^{13}\text{C-NMR}$  (126 MHz,  $\text{DMSO-}d_6$ ):  $\delta$  = 165.3, 156.5, 147.4, 129.2, 129.0, 126.2, 121.9, 121.2, 118.1, 116.0, 115.0, 114.1, 15.7. The signals for C-3'a and C-7'a were not detectable. Purity was determined with HPLC-MS to be  $\geq 95\%$  (m/z calculated for [M]: 282.36, found 283.1 for  $[\text{M} + \text{H}]^+$ ).

### 5.2.9. Preparation of salicylidene hydrazinobenzothiazoles (Figures 1, 2 box VI):

#### 5.2.9.1. 2-((2-(1',3'-benzothiazol-2'-yl)hydrazine-1-ylidene)methyl)phenol (6a)

The reaction of salicylic aldehyde (0.13 mL, 1.21 mmol) with 2-hydrazinobenzothiazole (200 mg, 1.21 mmol) in ethanolic solution under acetic acid catalysis delivered the pure product as a white precipitate in 93.3 % yield (306 mg, 1.13 mmol) after recrystallization. <sup>1</sup>H-NMR (500 MHz, DMSO-*d*<sub>6</sub>): δ = 12.14 (s, 1H), 10.44 (s, 1H), 8.45 (s, 1H), 7.74 (d, 1H, <sup>3</sup>*J*(H,H) = 7.9 Hz), 7.61 (d, 1H, <sup>3</sup>*J*(H,H) = 6.6 Hz), 7.41 – 7.32 (m, 1H), 7.31 – 7.27 (sm, 1H), 7.27 – 7.24 (sm, 1H), 7.09 (td, 1H, <sup>4</sup>*J*(H,H) = 1.3 Hz, <sup>3</sup>*J*(H,H) = 7.9 Hz), 6.95 – 6.88 (m, 2H). <sup>13</sup>C-NMR (126 MHz, DMSO-*d*<sub>6</sub>): δ = 166.4, 156.6, 147.0, 130.8, 127.7, 126.2, 121.8, 121.5, 119.6, 119.4, 116.1 – the signals for C-6', C-3'*a* and C-7'*a* were not visible. Anal. Calcd. for C<sub>14</sub>H<sub>11</sub>N<sub>3</sub>O: C: 62.43; H: 4.12; N: 15.60. Found: C: 62.56; H: 4.086; N: 15.76. Purity was additionally determined with HPLC-MS to be ≥ 95% (m/z calculated for [M]: 269.32, found 315.2 for [M + H]<sup>+</sup>).

#### 5.2.9.2. 2-(1-(2-(1',3'-benzothiazol-2'-yl)hydrazine-1-ylidene)ethyl)phenol (6b)

The reaction of 2-hydroxyacetophenon (0.15 mL, 1.21 mmol) with 2-hydrazinobenzothiazole (200 mg, 1.21 mmol) in ethanolic solution under acetic acid catalysis delivered the pure product as a yellow precipitate in 92 % yield (315 mg, 1.11 mmol) after recrystallization. <sup>1</sup>H-NMR (500 MHz, DMSO-*d*<sub>6</sub>): δ = 12.52 (bs, 1H), 7.66 (d, 1H, <sup>3</sup>*J*(H,H) = 7.7 Hz), 7.59 (dd, 1H, <sup>4</sup>*J*(H,H) = 1.0 Hz, <sup>3</sup>*J*(H,H) = 7.8 Hz), 7.30 – 7.24 (m, 2H), 7.19 (d, 1H, <sup>3</sup>*J*(H,H) = 7.8 Hz), 7.06 (t, 1H, <sup>3</sup>*J*(H,H) = 7.5 Hz), 6.93 – 6.87 (m, 2H), 6.50 (bs, 1H), 2.50 (s, 3H). <sup>13</sup>C-NMR (126 MHz, DMSO-*d*<sub>6</sub>): δ = 165.1, 159.6, 158.2, 141.2, 130.6, 128.4, 126.7, 123.7, 122.5, 121.6, 119.9, 118.7, 116.7, 112.4, 14.4. Anal. Calcd. for C<sub>15</sub>H<sub>13</sub>N<sub>3</sub>SO×1.25 H<sub>2</sub>O: C: 58.9; H: 5.11; N: 13.74. Found: C: 58.7; H: 4.728; N: 13.85.

### 5.2.10. Preparation of combined structures (Figures 1, 2, box VII):

#### 5.2.10.1. *N,N*-bis(4-methoxyphenyl)hydrazine-1,2-bis(carbothioamide) (7a)

The reaction of 4-methoxyphenylisothiocyanate (413.1 mg, 2.5 mmol) with hydrazine (0.06 mL 80% aqueous, 1.25 mmol) in ethanolic solution delivered the pure product as a white solid in 68.5 % yield (310 mg, 0.856 mmol) after recrystallization.

$^1\text{H-NMR}$  (500 MHz,  $\text{DMSO-}d_6$ ):  $\delta = 9.69$  (s, 2H), 9.52 (s, 2H), 7.38 (d, 4H,  $^3J(\text{H,H}) = 8.8$  Hz), 6.93 – 6.86 (m, 4H), 3.75 (s, 6H).  $^{13}\text{C-NMR}$  (126 MHz,  $\text{DMSO-}d_6$ ):  $\delta = 156.8$  (2C), 132.1 (2C), 126.8 (4C), 113.5 (4C), 55.35 (2C). – for the quaternary C=S no signal was visible in APT test, the signal at 126.8, which was assigned for C-2, C-2', C-6 and C-6' had a remarkably low intensity. Anal. Calcd. for  $\text{C}_{16}\text{H}_{18}\text{N}_4\text{S}_2\text{O}_2$ : C: 53.02; H: 5.01; N: 15.46. Found: C: 53.18; H: 5.047; N: 15.66.

#### 5.2.10.2. 3-[(1',3'-benzothiazol-2'-yl)amino]-1-(4-methoxyphenyl)thiourea (7b)

The reaction of *N*-(4-methoxyphenyl)hydrazinecarbothioamide **C-1** (250 mg, 1.513 mmol) with 2-hydrazinobenzothiazole (250 mg, 1.513 mmol) in ethanolic solution delivered the pure product as a yellow solid in 75 % yield (357.2 mg, 1.139 mmol) after recrystallization.

$^1\text{H-NMR}$  (500 MHz,  $\text{DMSO-}d_6$ ):  $\delta = 13.38$  (s, 1H), 7.66 (s, 1H), 7.60 (dd, 1H,  $^3J(\text{H,H}) = 1.3$  Hz,  $^3J(\text{H,H}) = 8.2$  Hz), 7.37 – 7.31 (sm, 1H), 7.30 – 7.25 (sm, 2H), 7.19 (dd, 1H,  $^3J(\text{H,H}) = 1.4$  Hz,  $^3J(\text{H,H}) = 7.7$  Hz), 7.10 – 7.06 (sm, 2H), 6.93 (td, 1H,  $^3J(\text{H,H}) = 1.4$  Hz,  $^3J(\text{H,H}) = 7.7$  Hz), 3.82 (s, 3H). For one NH no signal was visible.  $^{13}\text{C-NMR}$  (101 MHz,  $\text{DMSO-}d_6$ ):  $\delta = 165.7$ , 159.9, 148.4, 139.5, 133.5, 130.6, 129.7 (2C), 124.6, 124.5, 123.3, 119.6, 114.8 (2C), 55.6. Anal. Calcd. for  $\text{C}_{15}\text{H}_{14}\text{N}_4\text{S}_2\text{O}$ : C: 54.52; H: 4.27; N: 16.96. Found: C: 54.26; H: 4.082; N: 16.7.

#### 5.2.10.3. 3-(2-(1',3'-benzothiazol-2'-yl)hydrazine-1-ylidene)-2,3-dihydro-indol-2-one (7c)

The reaction of isatin (222.6 mg, 1.513 mmol) with 2-hydrazinobenzothiazole (250 mg, 1.513 mmol) in ethanolic solution under acetic acid catalysis delivered the pure product as a yellow precipitate after recrystallization (The yield was not determined).  $^1\text{H-NMR}$  (500 MHz,  $\text{DMSO-}d_6$ ):  $\delta$  = 13.38 (s, 1H), 11.24 (s, 1H), 7.94 (d, 1H,  $^3J(\text{H,H}) = 7.6$  Hz), 7.67 (d, 1H,  $^3J(\text{H,H}) = 7.6$  Hz), 7.55 (d, 1H,  $^3J(\text{H,H}) = 7.3$  Hz), 7.44 – 7.39 (sm, 1H), 7.39 – 7.34 (sm, 1H), 7.30 – 7.25 (m, 1H), 7.10 (t, 1H,  $^3J(\text{H,H}) = 7.7$  Hz), 6.97 (d, 1H,  $^3J(\text{H,H}) = 7.9$  Hz).  $^{13}\text{C-NMR}$  (126 MHz,  $\text{DMSO-}d_6$ ):  $\delta$  = 141.6, 130.9, 126.4, 123.3, 122.4, 121.9, 120.5, 120.0, 119.7, 111.1. Signals for *C-3*, *C-3a'*, and *C-7a'* were not visible in the APT test. Purity of the compound was determined with HPLC-MS to be  $\geq 95\%$  (m/z calculated for [M]: 294.33, found 295.2 for  $[\text{M} + \text{H}]^+$ ).

#### 5.2.10.4. 3-(2'-(6'-methoxypyrimidin-4'-yl)hydrazono)inulin-2-one (7d)

4-hydrazinyl-6-methoxypyrimidine necessary for the synthesis of **7d** was prepared as described earlier in a two-step approach starting from 4,6-dichloropyrimidine.[13,115]  $^1\text{H NMR}$  (500 MHz,  $\text{CDCl}_3$ ):  $\delta$  = 8.26 (s, 1H), 6.42 (bs, 1H), 6.07 (s, 1H), 3.92 (s, 3H), 3.42 (bs, 2H).  $^{13}\text{C NMR}$  (126 MHz,  $\text{CDCl}_3$ ):  $\delta$  = 170.7, 167.2, 157.7, 84.9, 53.9. The product (150 mg, 1.04 mmol) was then reacted with isatin (152.7 mg, 1.04 mmol) in ethanolic solution under acetic acid catalysis. The reaction delivered the pure product as a yellow powder after column chromatography and recrystallization in 23.9 % yield (68 mg, 0.248 mmol).  $^1\text{H-NMR}$  (500 MHz,  $\text{DMSO-}d_6$ ):  $\delta$  = 11.09 (bs, 1H), 10.70 (s, 1H), 8.51 (s, 1H), 8.11 (d, 1H,  $^3J(\text{H,H}) = 7.9$  Hz), 7.35 (td, 1H,  $^4J(\text{H,H}) = 0.9$  Hz,  $^3J(\text{H,H}) = 7.7$  Hz), 7.04 (td, 1H,  $^4J(\text{H,H}) = 0.9$  Hz,  $^3J(\text{H,H}) = 7.6$  Hz), 6.89 (d, 1H,  $^3J(\text{H,H}) = 7.9$  Hz), 6.63 (s, 1H), 3.93 (s, 3H).  $^{13}\text{C-NMR}$  (126 MHz,  $\text{DMSO-}d_6$ ):  $\delta$  = 170.2, 164.6, 163.1, 158.2, 143.1, 135.8, 131.7, 125.7, 121.5, 120.0, 110.9, 87.8, 53.9. Anal. Calcd. for  $\text{C}_{13}\text{H}_{11}\text{N}_5\text{O}\times\text{H}_2\text{O}$ : C: 54.35; H: 4.56;

N: 24.38. Found: C: 54.85; H: 4.517; N: 23.26. Additionally purity was determined with HPLC-MS to be  $\geq 95\%$  ( $m/z$  calculated for [M]: 269.26, found 270.0 for [M + H]<sup>+</sup>).

### 5.3. In Vitro testing

#### 5.3.1. Cell culture

The human ovarian carcinoma cell lines A2780 and the doxorubicin selected multidrug resistant counterpart A2780adr were obtained from ECACC, UK, (A2780: No. 93112519, A2780adr: No. 93112520), and cultivated in RPMI (Sigma Aldrich, Germany) supplemented with 10% fetal bovine serum and 50 unit/mL penicillin and streptomycin (Sigma Aldrich, Germany). Human foreskin fibroblast (HFF) cells were obtained from ATCC. HFF cells were cultured in DMEM supplemented with 10% FCS and 50 unit/mL penicillin and streptomycin. The human uterine sarcoma cell lines MES-SA and the doxorubicin selected MES-SA/Dx5 were obtained from ATCC (MES-SA: No. CRL-1976<sup>TM</sup>, MES-SA/Dx5: No. CRL-1977<sup>TM</sup>) and cultivated in DMEM (Sigma Aldrich, Hungary). The human cervix carcinoma cell line KB-3-1 and the vinblastine selected KB-V1 (kind gifts from Dr. Michael M. Gottesman, National Institutes of Health) were cultivated in DMEM. MES-SA and MES-SA/Dx5 cells expressing mCherry protein were engineered using a lentiviral system (Tóth *et al.*, in preparation). The phenotype of the resistant cells was verified using cytotoxicity assays (not shown). DMEM media (Sigma Aldrich, Hungary) were supplemented with 10% fetal bovine serum, 5 mmol/L glutamine, and 50 unit/mL penicillin and streptomycin (Life Technologies). All cell lines were cultivated at 37 °C, 5% CO<sub>2</sub>.

#### 5.3.2. MTT viability assay

MTT viability assays were performed as described earlier with minor modifications [13,27,116]. Briefly, cells were seeded into 96-well tissue culture plates (Sarstedt, Newton,

USA / Orange, Braine-l'Alleud, Belgium) in the appropriate density evaluated for each cell line (5000 cells per well for MES-SA/Dx5 and KB-3-1/V1 cells, 10000 cells per well for A2780 cells) and allowed to attach for 12 h. Test compounds were added to achieve the required final concentration in a final volume of 200  $\mu$ L per well. After an incubation period of 72 h, the supernatant was removed and fresh medium supplemented with the MTT reagent (0.83 mg/mL) was added. Incubation with MTT at 37 °C was terminated after 1 h by removing the supernatants and lysing the cells with 100  $\mu$ L DMSO per well. Viability of the cells was measured spectrophotometrically by absorbance at 540 nm using either a Perkin Elmer Victor X3, Perkin Elmer EnSpire, or a BMG POLARstar microplate reader. Data was background corrected by subtraction of the signal obtained from unstained cell lysates and normalized to untreated cells. Curves were fitted by Prism software [117] using the sigmoidal dose-response model (comparing variable and fixed slopes). Curve fit statistics were used to determine the concentration of test compound that resulted in 50% toxicity (IC<sub>50</sub>).

### **5.3.3. Fluorescent assay using mCherry transfected MES-SA and MES-SA/Dx5 cells**

Cells were seeded either on 96 or 384 well plates (Greiner bio-one, Hungary), using a volume of 100 or 40  $\mu$ L and a density of 5000 or 2500 cells per well and allowed to attach for 24 h. Dilutions of the test compounds were added to achieve the required final concentration in a final volume of 200  $\mu$ L per well for 96, and 60  $\mu$ L for 384 well plates. After a 72 h incubation period, fluorescence was measured using a PerkinElmer EnSpire Multimode Plate Reader at 585nm excitation and 610 nm emission wavelengths.

### **5.3.4. Calcein AM Assay**



The activity of P-gp was quantified by the Calcein AM assay [67]. Briefly, cells were stained with Calcein AM (Life Technologies, USA) in the presence or absence of the P-gp-inhibitor, verapamil, and then measured with a FACSCanto flow cytometer (BD Biosciences, USA). Dead cells were separated by TO-PRO@-3 DNA dye staining (Life Technologies, USA). To evaluate the effect of the compounds on the functional expression of P-gp, MES-SA/Dx5 cells were cultured for five days in the presence of selected compounds at IC<sub>20</sub> concentrations, as calculated from viability assays. Fresh medium was added without the drugs every fifth day to support recovery. Functional expression of P-gp was evaluated by the Calcein AM assay when the cells reached 80% confluency.

### **5.3.5. Immunocytochemistry**

Cells were plated onto 8-well chambers (Nunc Lab-Tek II chamber slide system, Thermo Scientific). After 1 day, cells were fixed with 4% paraformaldehyde in Dulbecco's modified phosphate-buffered saline (DPBS) for 15 min at room temperature. After three washing steps with DPBS, nonspecific antibody binding was blocked for 1 h at room temperature in DBS containing 2 mg/mL BSA, 1% fish gelatin, 5% goat serum, and 0.1% Triton-X 100. The samples were then incubated with anti-P-gp (monoclonal anti-human MRK16, Kamiya Biomedical) primary antibody in blocking solution at a 1:500 dilution for 1 h at room temperature. After washing with DPBS, the cells were incubated for 1 h with Phycoerithrin-conjugated goat anti-mouse IgG (Invitrogen) secondary antibody in blocking solution at 1:250 dilution at room temperature. Secondary antibodies were diluted in the blocking solution at 1:250 in each case. Phycoerithrin-conjugated goat anti-mouse IgG antibody (Invitrogen) was applied to detect P-glycoprotein. DAPI (Invitrogen) was used for nuclear staining (1  $\mu$ M, 10 min long incubation in DPBS). The stained samples were examined by an Axioscope 2

fluorescent microscope (Zeiss, Thornwood, NY) and a Zeiss LSM 710 confocal laser scanning microscope.

#### **5.4. Analysis of DTP data**

Substructure searches for NNS and ONS chelators were performed on the DTP database using the Instant J Chem software package from Chemaxon [56]. The resulting compounds were visually inspected for presence of metal ions and the ability to chelate. Numbers of search results and compounds with available biodata are given in the supporting information (Figure S12). Results were refined by an additional substructure search distinguishing between imino methylated and desmethylated derivatives. Numbers of these refinements are given in Figure S13. For the general comparison of toxicity (Figures 9D, S9), the data on all 60 cell lines was averaged for each compound.

#### **6. Author Contributions**

The manuscript was written through contributions of all authors. VFSP conceived the study, designed, synthesized and tested the compounds; SzT performed fluorescent toxicity assays; AF and KSz performed immunostaining following long time incubation assays; AL performed bioinformatic analysis; PSz performed HPLC-MS measurements, VFSP, MW and GSz analyzed the data and wrote the manuscript. All authors approved the final version of the manuscript.

#### **7. Acknowledgements**

We thank Éva Anna Enyedy and Norbert Szoboszlai for the critical reading of the manuscript. VFSP thanks Sarah Hopp, Christian Müller and Roland Pietz for support in the synthesis,

Elvira Komlósi for technical assistance, Katalin Kiss for support with confocal microscopy, as well as Judit Sessler for fruitful discussions.

## 8. Funding Sources

GS was supported by a Momentum Grant of the Hungarian Academy of Sciences. Funding from ERC (StG-260572) and NKTH-ANR 10-1-2011-0401 is also acknowledged.

## 9. References

- [1] P. Chiba, G.F. Ecker, Inhibitors of ABC-type drug efflux pumps: an overview of the current patent situation, *Expert Opin. Ther. Pat.* 14 (2004) 499–508.  
doi:10.1517/13543776.14.4.499.
- [2] P. Boyle, B. Levin, International Agency for Research on Cancer., *World cancer report 2008 2008*, IARC Press, Lyon, 2008. <http://site.ebrary.com/id/10306279> (accessed November 18, 2014).
- [3] M.M. Gottesman, T. Fojo, S.E. Bates, MULTIDRUG RESISTANCE IN CANCER: ROLE OF ATP-DEPENDENT TRANSPORTERS, *Nat. Rev. Cancer.* 2 (2002) 48–58.  
doi:10.1038/nrc706.
- [4] G.J. Schuurhuis, H.J. Broxterman, J.H. de Lange, H.M. Pinedo, T.H. van Heijningen, C.M. Kuiper, et al., Early multidrug resistance, defined by changes in intracellular doxorubicin distribution, independent of P-glycoprotein., *Br. J. Cancer.* 64 (1991) 857–861.
- [5] K. Aktories, U. Förstermann, F. Hofmann, K. Starke, *Allgemeine und spezielle Pharmakologie und Toxikologie*, 9th ed., Elsevier, 2005.

- [6] G. Szakács, J.K. Paterson, J.A. Ludwig, C. Booth-Genthe, M.M. Gottesman, Targeting multidrug resistance in cancer, *Nat. Rev. Drug Discov.* 5 (2006) 219–234.  
doi:10.1038/nrd1984.
- [7] B. Marquez, F. Van Bambeke, ABC multidrug transporters: target for modulation of drug pharmacokinetics and drug-drug interactions, *Curr. Drug Targets.* 12 (2011) 600–620.
- [8] M. Whitnall, J. Howard, P. Ponka, D.R. Richardson, A class of iron chelators with a wide spectrum of potent antitumor activity that overcomes resistance to chemotherapeutics, *Proc. Natl. Acad. Sci.* 103 (2006) 14901–14906.
- [9] A.M. Merlot, D.S. Kalinowski, D.R. Richardson, Novel Chelators for Cancer Treatment: Where Are We Now?, *Antioxid. Redox Signal.* 18 (2013) 973–1006.  
doi:10.1089/ars.2012.4540.
- [10] N.T.V. Le, D.R. Richardson, The role of iron in cell cycle progression and the proliferation of neoplastic cells, *Biochim. Biophys. Acta BBA - Rev. Cancer.* 1603 (2002) 31–46. doi:10.1016/S0304-419X(02)00068-9.
- [11] A. Gaál, G. Orgován, Z. Polgári, A. Réti, V.G. Mihucz, S. Bősze, et al., Complex forming competition and in-vitro toxicity studies on the applicability of di-2-pyridylketone-4,4,-dimethyl-3-thiosemicarbazone (Dp44mT) as a metal chelator, *J. Inorg. Biochem.* 130 (2014) 52–58. doi:10.1016/j.jinorgbio.2013.09.016.
- [12] D.S. Kalinowski, D.R. Richardson, The Evolution of Iron Chelators for the Treatment of Iron Overload Disease and Cancer, *Pharmacol. Rev.* 57 (2005) 547–583.  
doi:10.1124/pr.57.4.2.
- [13] V.F.S. Pape, D. Türk, P. Szabó, M. Wiese, E.A. Enyedy, G. Szakács, Synthesis and characterization of the anticancer and metal binding properties of novel

- pyrimidinylhydrazone derivatives, *J. Inorg. Biochem.* 144 (2015) 18–30.  
doi:10.1016/j.jinorgbio.2014.12.015.
- [14] D.J.R. Lane, T.M. Mills, N.H. Shafie, A.M. Merlot, R. Saleh Moussa, D.S. Kalinowski, et al., Expanding horizons in iron chelation and the treatment of cancer: Role of iron in the regulation of ER stress and the epithelial–mesenchymal transition, *Biochim. Biophys. Acta BBA - Rev. Cancer.* 1845 (2014) 166–181.  
doi:10.1016/j.bbcan.2014.01.005.
- [15] D. Türk, M.D. Hall, B.F. Chu, J.A. Ludwig, H.M. Fales, M.M. Gottesman, et al., Identification of Compounds Selectively Killing Multidrug-Resistant Cancer Cells, *Cancer Res.* 69 (2009) 8293–8301. doi:10.1158/0008-5472.CAN-09-2422.
- [16] R.W. Brockman, J.R. Thomson, M.J. Bell, H.E. Skipper, Observations on the Antileukemic Activity of Pyridine-2-carboxaldehyde Thiosemicarbazone and Thiocarbohydrazone, *Cancer Res.* 16 (1956) 167–170.
- [17] C.R. Kowol, R. Berger, R. Eichinger, A. Roller, M.A. Jakupec, P.P. Schmidt, et al., Gallium(III) and Iron(III) Complexes of  $\alpha$ -N-Heterocyclic Thiosemicarbazones: Synthesis, Characterization, Cytotoxicity, and Interaction with Ribonucleotide Reductase, *J. Med. Chem.* 50 (2007) 1254–1265. doi:10.1021/jm0612618.
- [18] Y. Yu, J. Wong, D.B. Lovejoy, D.S. Kalinowski, D.R. Richardson, Chelators at the Cancer Coalface: Desferrioxamine to Triapine and Beyond, *Clin. Cancer Res.* 12 (2006) 6876–6883. doi:10.1158/1078-0432.CCR-06-1954.
- [19] C.M. Nutting, C.M.L. van Herpen, A.B. Miah, S.A. Bhide, J.-P. Machiels, J. Buter, et al., Phase II study of 3-AP Triapine in patients with recurrent or metastatic head and neck squamous cell carcinoma, *Ann. Oncol.* 20 (2009) 1275–1279.  
doi:10.1093/annonc/mdn775.

- [20] G. Rappa, A. Lorico, M.-C. Liu, G.D. Kruh, A.H. Cory, J.G. Cory, et al., Overexpression of the Multidrug Resistance Genes *mdr1*, *mdr3*, and *mrp* in L1210 Leukemia Cells Resistant to Inhibitors of Ribonucleotide Reductase, *Biochem. Pharmacol.* 54 (1997) 649–655.
- [21] M.D. Hall, N.K. Salam, J.L. Hellawell, H.M. Fales, C.B. Kensler, J.A. Ludwig, et al., Synthesis, Activity, and Pharmacophore Development for Isatin- $\beta$ -thiosemicarbazones with Selective Activity toward Multidrug-Resistant Cells, *J. Med. Chem.* 52 (2009) 3191–3204. doi:10.1021/jm800861c.
- [22] C.R. Kowol, R. Trondl, P. Heffeter, V.B. Arion, M.A. Jakupec, A. Roller, et al., Impact of Metal Coordination on Cytotoxicity of 3-Aminopyridine-2-carboxaldehyde Thiosemicarbazone (Triapine) and Novel Insights into Terminal Dimethylation, *J. Med. Chem.* 52 (2009) 5032–5043. doi:10.1021/jm900528d.
- [23] P.V. Bernhardt, P.C. Sharpe, M. Islam, D.B. Lovejoy, D.S. Kalinowski, D.R. Richardson, Iron Chelators of the Dipyridylketone Thiosemicarbazone Class: Precomplexation and Transmetalation Effects on Anticancer Activity, *J. Med. Chem.* 52 (2009) 407–415. doi:10.1021/jm801012z.
- [24] P.J. Jansson, T. Yamagishi, A. Arvind, N. Seebacher, E. Gutierrez, A. Stacy, et al., Di-2-pyridylketone 4,4-Dimethyl-3-thiosemicarbazone (Dp44mT) Overcomes Multidrug-Resistance by a Novel Mechanism Involving the Hijacking of Lysosomal P-Glycoprotein (Pgp)., *J. Biol. Chem.* 290 (2015) 9588–9603. doi:10.1074/jbc.M114.631283.
- [25] A. Tamaki, C. Ierano, G. Szakács, R.W. Robey, S.E. Bates, The controversial role of ABC transporters in clinical oncology, *Essays Biochem.* 50 (2011) 209–232. doi:10.1042/bse0500209.

- [26] K. Juvale, M. Wiese, 4-Substituted-2-phenylquinazolines as inhibitors of BCRP, *Bioorg. Med. Chem. Lett.* 22 (2012) 6766–6769. doi:10.1016/j.bmcl.2012.08.024.
- [27] K. Juvale, V.F.S. Pape, M. Wiese, Investigation of chalcones and benzochalcones as inhibitors of breast cancer resistance protein, *Bioorg. Med. Chem.* 20 (2012) 346–355. doi:10.1016/j.bmc.2011.10.074.
- [28] J.D. Allen, A. van Loevezijn, J.M. Lakhai, M. van der Valk, O. van Tellingen, G. Reid, et al., Potent and Specific Inhibition of the Breast Cancer Resistance Protein Multidrug Transporter in Vitro and in Mouse Intestine by a Novel Analogue of Fumitremorgin C  
1 This work was supported in part by grant NKI 97-1433 from the Dutch Cancer Society (to A. H. S.). Synthesis investigations by A. v. L. and G-J. K. were supported by the Netherlands Research Council for Chemical Sciences (NWO/CW) and the Netherlands Technology Foundation (STW).1, *Mol. Cancer Ther.* 1 (2002) 417–425.
- [29] I. Ivnitiski-Steele, R.S. Larson, D.M. Lovato, H.M. Khawaja, S.S. Winter, T.I. Oprea, et al., High-Throughput Flow Cytometry to Detect Selective Inhibitors of ABCB1, ABCC1, and ABCG2 Transporters, *ASSAY Drug Dev. Technol.* 6 (2008) 263–276. doi:10.1089/adt.2007.107.
- [30] P. Matsson, J.M. Pedersen, U. Norinder, C.A.S. Bergström, P. Artursson, Identification of Novel Specific and General Inhibitors of the Three Major Human ATP-Binding Cassette Transporters P-gp, BCRP and MRP2 Among Registered Drugs, *Pharm. Res.* 26 (2009) 1816–1831. doi:10.1007/s11095-009-9896-0.
- [31] Z. Shi, A.K. Tiwari, S. Shukla, R.W. Robey, S. Singh, I.-W. Kim, et al., Sildenafil Reverses ABCB1- and ABCG2-Mediated Chemotherapeutic Drug Resistance, *Cancer Res.* 71 (2011) 3029–3041. doi:10.1158/0008-5472.CAN-10-3820.

- [32] E. Bakos, R. Evers, E. Sinkó, A. Váradi, P. Borst, B. Sarkadi, Interactions of the human multidrug resistance proteins MRP1 and MRP2 with organic anions, *Mol. Pharmacol.* 57 (2000) 760–768.
- [33] S. Shukla, C.-P. Wu, S.V. Ambudkar, Development of inhibitors of ATP-binding cassette drug transporters – present status and challenges, *Expert Opin. Drug Metab. Toxicol.* 4 (2008) 205–223. doi:10.1517/17425255.4.2.205.
- [34] O. Polgar, S.E. Bates, ABC transporters in the balance: is there a role in multidrug resistance?, *Biochem. Soc. Trans.* 33 (2005) 241–246.
- [35] G. Szakács, G.K. Chen, M.M. Gottesman, The molecular mysteries underlying P-glycoprotein-mediated multidrug resistance, *Cancer Biol. Ther.* 3 (2004) 382–384.
- [36] M. Falasca, K.J. Linton, Investigational ABC transporter inhibitors, *Expert Opin. Investig. Drugs.* 21 (2012) 657–666. doi:10.1517/13543784.2012.679339.
- [37] M. Yu, A. Ocana, I.F. Tannock, Reversal of ATP-binding cassette drug transporter activity to modulate chemoresistance: why has it failed to provide clinical benefit?, *Cancer Metastasis Rev.* 32 (2013) 211–227. doi:10.1007/s10555-012-9402-8.
- [38] L. Amiri-Kordestani, A. Basseville, K. Kurdziel, A.T. Fojo, S.E. Bates, Targeting MDR in breast and lung cancer: Discriminating its potential importance from the failure of drug resistance reversal studies, *Drug Resist. Updat.* 15 (2012) 50–61. doi:10.1016/j.drug.2012.02.002.
- [39] G. Szakács, M.D. Hall, M.M. Gottesman, A. Boumendjel, R. Kachadourian, B.J. Day, et al., Targeting the Achilles Heel of Multidrug-Resistant Cancer by Exploiting the Fitness Cost of Resistance, *Chem. Rev.* 114 (2014) 5753–5774. doi:10.1021/cr4006236.



- [40] G. Szakács, J.-P. Annereau, S. Lababidi, U. Shankavaram, A. Arciello, K.J. Bussey, et al., Predicting drug sensitivity and resistance: profiling ABC transporter genes in cancer cells, *Cancer Cell*. 6 (2004) 129–137.
- [41] W.C. Reinhold, M. Sunshine, H. Liu, S. Varma, K.W. Kohn, J. Morris, et al., CellMiner: A Web-Based Suite of Genomic and Pharmacologic Tools to Explore Transcript and Drug Patterns in the NCI-60 Cell Line Set, *Cancer Res.* 72 (2012) 3499–3511. doi:10.1158/0008-5472.CAN-12-1370.
- [42] R.H. Shoemaker, The NCI60 human tumour cell line anticancer drug screen, *Nat. Rev. Cancer*. 6 (2006) 813–823. doi:10.1038/nrc1951.
- [43] J.A. Ludwig, G. Szakács, S.E. Martin, B.F. Chu, C. Cardarelli, Z.E. Sauna, et al., Selective Toxicity of NSC73306 in MDR1-Positive Cells as a New Strategy to Circumvent Multidrug Resistance in Cancer, *Cancer Res.* 66 (2006) 4808–4815. doi:10.1158/0008-5472.CAN-05-3322.
- [44] M.D. Hall, K.R. Brimacombe, M.S. Varonka, K.M. Pluchino, J.K. Monda, J. Li, et al., Synthesis and Structure–Activity Evaluation of Isatin- $\beta$ -thiosemicarbazones with Improved Selective Activity toward Multidrug-Resistant Cells Expressing P-Glycoprotein, *J. Med. Chem.* 54 (2011) 5878–5889. doi:10.1021/jm2006047.
- [45] I. Machado, M. Fernández, L. Becco, B. Garat, R.F. Brissos, N. Zabarska, et al., New metal complexes of NNO tridentate ligands: Effect of metal center and co-ligand on biological activity, *Inorganica Chim. Acta.* 420 (2014) 39–46. doi:10.1016/j.ica.2013.10.022.
- [46] M. Calinescu, E. Ion, R. Georgescu, T. Negreanu-prjol, Synthesis and spectroscopic, antibacterial and antifungal studies on copper (II) complexes with 2-benzothiazolyl hydrazones, *Rev Roum Chim.* 53 (2008) 911–919.

- [47] D.R. Richardson, P.C. Sharpe, D.B. Lovejoy, D. Senaratne, D.S. Kalinowski, M. Islam, et al., Dipyriddy Thiosemicarbazone Chelators with Potent and Selective Antitumor Activity Form Iron Complexes with Redox Activity, *J. Med. Chem.* 49 (2006) 6510–6521. doi:10.1021/jm0606342.
- [48] W. Miklos, K. Pelivan, C.R. Kowol, C. Pirker, R. Dornetshuber-Fleiss, M. Spitzwieser, et al., Triapine-mediated ABCB1 induction via PKC induces widespread therapy unresponsiveness but is not underlying acquired triapine resistance, *Cancer Lett.* 361 (2015) 112–120. doi:10.1016/j.canlet.2015.02.049.
- [49] J. Easmon, G. Heinisch, J. Hofmann, T. Langer, H. Grunicke, J. Fink, et al., Thiazolyl and benzothiazolyl hydrazones derived from  $\alpha$ -(N)-acetylpyridines and diazines: synthesis, antiproliferative activity and CoMFA studies, *Eur. J. Med. Chem.* 32 (1997) 397–408. doi:10.1016/S0223-5234(97)81677-7.
- [50] J. Easmon, G. Pürstinger, K.-S. Thies, G. Heinisch, J. Hofmann, *Synthesis, Structure–Activity Relationships, and Antitumor Studies of 2-Benzoxazolyl Hydrazones Derived from Alpha-( N )-acyl Heteroaromatics*, *J. Med. Chem.* 49 (2006) 6343–6350. doi:10.1021/jm060232u.
- [51] E.M. Becker, D.B. Lovejoy, J.M. Greer, R. Watts, D.R. Richardson, Identification of the di-pyridyl ketone isonicotinoyl hydrazone (PKIH) analogues as potent iron chelators and anti-tumour agents, *Br. J. Pharmacol.* 138 (2003) 819–830. doi:10.1038/sj.bjp.0705089.
- [52] K. Ishiguro, Z.P. Lin, P.G. Penketh, K. Shyam, R. Zhu, R.P. Baumann, et al., Distinct mechanisms of cell-kill by triapine and its terminally dimethylated derivative Dp44mT due to a loss or gain of activity of their copper(II) complexes, *Biochem. Pharmacol.* 91 (2014) 312–322. doi:10.1016/j.bcp.2014.08.006.

- [53] N.S. Youssef, E. El-Zahany, A.M.A. El-Seidy, A. Caselli, S. Fantauzzi, S. Cenini, Synthesis and characterisation of new Schiff base metal complexes and their use as catalysts for olefin cyclopropanation, *Inorganica Chim. Acta.* 362 (2009) 2006–2014. doi:10.1016/j.ica.2008.09.012.
- [54] I.H. Hall, N.J. Peaty, J.R. Henry, J. Easmon, G. Heinisch, G. Pürstinger, Investigations on the mechanism of action of the novel antitumor agents 2-benzothiazolyl, 2-benzoxazolyl, and 2-benzimidazolyl hydrazones derived from 2-acetylpyridine, *Arch. Pharm. (Weinheim).* 332 (1999) 115–123.
- [55] K.J. Schaper, J.K. Seydel, M. Rosenfeld, J. Kazda, Development of inhibitors of mycobacterial ribonucleotide reductase, *Lepr. Rev.* 57 Suppl 3 (1986) 254–264.
- [56] L. ChemAxon, Instant J Chem / MarvinSketch, ChemAxon Ltd., Budapest, Hungary, 2012. <http://www.chemaxon.com>.
- [57] C.M. Beaufort, J.C.A. Helmijr, A.M. Piskorz, M. Hoogstraat, K. Ruigrok-Ritstier, N. Besselink, et al., Ovarian Cancer Cell Line Panel (OCCP): Clinical Importance of In Vitro Morphological Subtypes, *PLoS ONE.* 9 (2014) e103988. doi:10.1371/journal.pone.0103988.
- [58] W.G. Harker, B.I. Sikic, Multidrug (Pleiotropic) Resistance in Doxorubicin-selected Variants of the Human Sarcoma Cell Line MES-SA, *Cancer Res.* 45 (1985) 4091–4096.
- [59] E. Wang, M.D. Lee, K.W. Dunn, Lysosomal accumulation of drugs in drug-sensitive MES-SA but not multidrug-resistant MES-SA/Dx5 uterine sarcoma cells, *J. Cell. Physiol.* 184 (2000) 263–274. doi:10.1002/1097-4652(200008)184:2<263::AID-JCP15>3.0.CO;2-F.
- [60] D.-W. Shen, C. Cardarelli, J. Hwang, M. Cornwell, N. Richert, S. Ishii, et al., Multiple drug-resistant human KB carcinoma cells independently selected for high-level

- resistance to colchicine, adriamycin, or vinblastine show changes in expression of specific proteins., *J. Biol. Chem.* 261 (1986) 7762–7770.
- [61] J. Wang, L.-S. Tai, C.-H. Tzang, W.F. Fong, X.-Y. Guan, M. Yang, 1p31, 7q21 and 18q21 chromosomal aberrations and candidate genes in acquired vinblastine resistance of human cervical carcinoma KB cells, *Oncol. Rep.* 19 (2008) 1155–1164.
- [62] G. Elliott, J. McGrath, E. Crockett-Torabi, Green Fluorescent Protein: A Novel Viability Assay for Cryobiological Applications, *Cryobiology.* 40 (2000) 360–369. doi:10.1006/cryo.2000.2258.
- [63] K.R. Brimacombe, M.D. Hall, D.S. Auld, J. Inglese, C.P. Austin, M.M. Gottesman, et al., A Dual-Fluorescence High-Throughput Cell Line System for Probing Multidrug Resistance, *Assay Drug Dev. Technol.* 7 (2009) 233–249. doi:10.1089/adt.2008.165.
- [64] C. Baumstark-Khan, M. Palm, J. Wehner, M. Okabe, M. Ikawa, G. Horneck, Green Fluorescent Protein (GFP) as a Marker for Cell Viability After UV Irradiation, *J. Fluoresc.* 9 (1999) 37–43. doi:10.1023/A:1020583623407.
- [65] J.B. Baell, G.A. Holloway, New Substructure Filters for Removal of Pan Assay Interference Compounds (PAINS) from Screening Libraries and for Their Exclusion in Bioassays, *J. Med. Chem.* 53 (2010) 2719–2740. doi:10.1021/jm901137j.
- [66] J. Baell, M.A. Walters, Chemistry: Chemical con artists foil drug discovery, *Nat. News.* 513 (2014) 481. doi:10.1038/513481a.
- [67] L. Homolya, M. Holló, M. Müller, E.B. Mechetner, B. Sarkadi, A new method for a quantitative assessment of P-glycoprotein-related multidrug resistance in tumour cells., *Br. J. Cancer.* 73 (1996) 849–855.
- [68] D.L. Klayman, J.F. Bartosevich, T.S. Griffin, C.J. Mason, J.P. Scovill, 2-Acetylpyridine thiosemicarbazones. 1. A new class of potential antimalarial agents, *J. Med. Chem.* 22 (1979) 855–862.

- [69] D. Gupta-Ostermann, J. Bajorath, The “SAR Matrix” method and its extensions for applications in medicinal chemistry and chemogenomics, *F1000Research*. (2014). doi:10.12688/f1000research.4185.2.
- [70] A. Budimir, Metal ions, Alzheimer’s disease and chelation therapy, *Acta Pharm.* 61 (2011) 1–14. doi:10.2478/v10007-011-0006-6.
- [71] K.M. Pluchino, M.D. Hall, A.S. Goldsborough, R. Callaghan, M.M. Gottesman, Collateral sensitivity as a strategy against cancer multidrug resistance, *Drug Resist. Updat.* 15 (2012) 98–105. doi:10.1016/j.drug.2012.03.002.
- [72] M.D. Hall, M.D. Handley, M.M. Gottesman, Is resistance useless? Multidrug resistance and collateral sensitivity, *Trends Pharmacol. Sci.* 30 (2009) 546–556. doi:10.1016/j.tips.2009.07.003.
- [73] A.S. Goldsborough, M.D. Handley, A.E. Dulcey, K.M. Pluchino, P. Kannan, K.R. Brimacombe, et al., Collateral Sensitivity of Multidrug-Resistant Cells to the Orphan Drug Tiopronin, *J. Med. Chem.* 54 (2011) 4987–4997. doi:10.1021/jm2001663.
- [74] M.D. Hall, T.S. Marshall, A.D.T. Kwit, L.M.M. Jenkins, A.E. Dulcey, J.P. Madigan, et al., Inhibition of Glutathione Peroxidase Mediates the Collateral Sensitivity of Multidrug-Resistant Cells to Tiopronin, *J. Biol. Chem.* (2014) jbc.M114.581702. doi:10.1074/jbc.M114.581702.
- [75] K.M. Marks, E.S. Park, A. Arefolov, K. Russo, K. Ishihara, J.E. Ring, et al., The Selectivity of Austocystin D Arises from Cell-Line-Specific Drug Activation by Cytochrome P450 Enzymes, *J. Nat. Prod.* 74 (2011) 567–573. doi:10.1021/np100429s.
- [76] J. Bentley, D.M. Quinn, R.S. Pitman, J.R. Warr, G.L. Kellett, The human KB multidrug-resistant cell line KB-C1 is hypersensitive to inhibitors of glycosylation, *Cancer Lett.* 115 (1997) 221–227.

- [77] S.E. Bell, D.M. Quinn, G.L. Kellett, J.R. Warr, 2-Deoxy-D-glucose preferentially kills multidrug-resistant human KB carcinoma cell lines by apoptosis., *Br. J. Cancer.* 78 (1998) 1464–1470.
- [78] H.J. Broxterman, H.M. Pinedo, C.M. Kuiper, L.C. Kaptein, G.J. Schuurhuis, J. Lankelma, Induction by verapamil of a rapid increase in ATP consumption in multidrug-resistant tumor cells., *FASEB J.* 2 (1988) 2278–2282.
- [79] H.J. Broxterman, H.M. Pinedo, C.M. Kuiper, G.J. Schuurhuis, J. Lankelma, Glycolysis in P-glycoprotein-overexpressing human tumor cell lines Effects of resistance-modifying agents, *FEBS Lett.* 247 (1989) 405–410. doi:10.1016/0014-5793(89)81380-8.
- [80] J.R. Warr, F. Brewer, M. Anderson, J. Fergusson, Verapamil hypersensitivity of vincristine resistant Chinese hamster ovary cell lines, *Cell Biol. Int. Rep.* 10 (1986) 389–399. doi:10.1016/0309-1651(86)90011-1.
- [81] E. Landwojtowicz, P. Nervi, A. Seelig, Real-Time Monitoring of P-Glycoprotein Activation in Living Cells <sup>†</sup>, *Biochemistry (Mosc.)*. 41 (2002) 8050–8057. doi:10.1021/bi025720s.
- [82] E. Gatlik-Landwojtowicz, P. Äänismaa, A. Seelig, The Rate of P-Glycoprotein Activation Depends on the Metabolic State of the Cell <sup>†</sup>, *Biochemistry (Mosc.)*. 43 (2004) 14840–14851. doi:10.1021/bi048761s.
- [83] J. Karwatsky, M.C. Lincoln, E. Georges, A mechanism for P-glycoprotein-mediated apoptosis as revealed by verapamil hypersensitivity, *Biochemistry (Mosc.)*. 42 (2003) 12163–12173.
- [84] J. Kotz, Phenotypic screening, take two, *SciBX Sci.-Bus. Exch.* 5 (2012). doi:10.1038/scibx.2012.380.

- [85] J.A. Lee, M.T. Uhlik, C.M. Moxham, D. Tomandl, D.J. Sall, Modern Phenotypic Drug Discovery Is a Viable, Neoclassic Pharma Strategy, *J. Med. Chem.* 55 (2012) 4527–4538. doi:10.1021/jm201649s.
- [86] A.S. Dobek, D.L. Klayman, E.T. Dickson, J.P. Scovill, E.C. Tramont, Inhibition of clinically significant bacterial organisms in vitro by 2-acetylpyridine thiosemicarbazones., *Antimicrob. Agents Chemother.* 18 (1980) 27–36. doi:10.1128/AAC.18.1.27.
- [87] X. Mei, P. Wang, A. Caracoti, P. Mingo, V. Boyd, R. Murray, et al., Hydrazone, hydrazine and thiosemicarbazone derivatives as antifungal agents, Google Patents, 2001. <http://www.google.com/patents/US6329378> (accessed September 29, 2014).
- [88] D.X. West, J.J. Ingram III, N.M. Kozub, G.A. Bain, A.E. Liberta, Copper (II) complexes of 2-formyl-, 2-acetyl- and 2-benzoyl-pyridine N (4)-phenyl-, N (4)-o-methoxyphenyl-, N (4)-p-methoxy-phenyl- and N (4)-p-nitrophenylthiosemicarbazones, *Transit. Met. Chem.* 21 (1996) 213–218.
- [89] M.A. Soares, J.A. Lessa, I.C. Mendes, J.G. Da Silva, R.G. dos Santos, L.B. Salum, et al., N4-Phenyl-substituted 2-acetylpyridine thiosemicarbazones: Cytotoxicity against human tumor cells, structure–activity relationship studies and investigation on the mechanism of action, *Bioorg. Med. Chem.* 20 (2012) 3396–3409. doi:10.1016/j.bmc.2012.04.027.
- [90] J.A. Lessa, I.C. Mendes, P.R.O. da Silva, M.A. Soares, R.G. dos Santos, N.L. Speziali, et al., 2-Acetylpyridine thiosemicarbazones: Cytotoxic activity in nanomolar doses against malignant gliomas, *Eur. J. Med. Chem.* 45 (2010) 5671–5677. doi:10.1016/j.ejmech.2010.09.021.
- [91] P. Sengupta, R. Dinda, S. Ghosh, Ruthenium(II) complexes of NSO donor ligands in the form of ring-substituted 4-phenyl-thiosemicarbazones of salicylaldehyde and o-

- hydroxyacetophenone, *Transit. Met. Chem.* 27 (2002) 665–667.  
doi:10.1023/A:1019800729485.
- [92] V. Mahalingam, N. Chitrapriya, F.R. Fronczek, K. Natarajan, New Ru(II)–DMSO complexes of ON/SN chelates: Synthesis, behavior of Schiff bases towards hydrolytic cleavage of CN bond, electrochemistry and biological activities, *Polyhedron*. 29 (2010) 3363–3371. doi:10.1016/j.poly.2010.09.019.
- [93] E.B. Seena, M.R.P. Kurup, Spectral and structural studies of mono- and binuclear copper(II) complexes of salicylaldehyde N(4)-substituted thiosemicarbazones, *Polyhedron*. 26 (2007) 829–836. doi:10.1016/j.poly.2006.09.040.
- [94] P. Bindu, M.R.P. Kurup, T.R. Satyakeerty, Epr, cyclic voltammetric and biological activities of copper(II) complexes of salicylaldehyde N(4)-substituted thiosemicarbazone and heterocyclic bases, *Polyhedron*. 18 (1998) 321–331.  
doi:10.1016/S0277-5387(98)00166-1.
- [95] E. Pahontu, V. Fala, A. Gulea, D. Poirier, V. Tapcov, T. Rosu, Synthesis and Characterization of Some New Cu(II), Ni(II) and Zn(II) Complexes with Salicylidene Thiosemicarbazones: Antibacterial, Antifungal and in Vitro Antileukemia Activity, *Molecules*. 18 (2013) 8812–8836. doi:10.3390/molecules18088812.
- [96] Saswati, R. Dinda, C.S. Schmiesing, E. Sinn, Y.P. Patil, M. Nethaji, et al., Mixed-ligand nickel(II) thiosemicarbazone complexes: Synthesis, characterization and biological evaluation, *Polyhedron*. 50 (2013) 354–363. doi:10.1016/j.poly.2012.11.031.
- [97] I. Đilović, M. Rubčić, V. Vrdoljak, S.K. Pavelić, M. Kralj, I. Piantanida, et al., Novel thiosemicarbazone derivatives as potential antitumor agents: Synthesis, physicochemical and structural properties, DNA interactions and antiproliferative activity, *Bioorg. Med. Chem.* 16 (2008) 5189–5198. doi:10.1016/j.bmc.2008.03.006.



- [98] S.A. Thompson, L. Wheat, N.A. Brown, P.B. Wingrove, G.V. Pillai, P.J. Whiting, et al., Salicylidene salicylhydrazide, a selective inhibitor of  $\beta$  1-containing GABA<sub>A</sub> receptors, *Br. J. Pharmacol.* 142 (2004) 97–106. doi:10.1038/sj.bjp.0705689.
- [99] K. Krishnan, K. Prathiba, V. Jayaprakash, A. Basu, N. Mishra, B. Zhou, et al., Synthesis and ribonucleotide reductase inhibitory activity of thiosemicarbazones, *Bioorg. Med. Chem. Lett.* 18 (2008) 6248–6250. doi:10.1016/j.bmcl.2008.09.097.
- [100] E. Ion, M. Calinescu, A. Emandi, V. Badea, D. Negoiu, Copper (II) Complex Compounds with Mixed Hydrazone Ligands, *Rev. Chim.-Buchar.-Orig. Ed.-.* 59 (2008) 12.
- [101] A. Shaikh Kabber, M.A. Bassar, N.A. Mote, Synthesis and Antimicrobial Activity of Some Schiff Bases from Benzothiazoles, *Asian J. Chem.* 13 (2001) 496–500.
- [102] M. Călinescu, E. Ion, A.-M. Stadler, Studies on nickel (II) complex compounds with 2-benzothiazolyl hydrazones, *Rev Roum Chim.* 53 (2008) 903–909.
- [103] E.B. Lindgren, M.A. de Brito, T.R.A. Vasconcelos, M.O. de Moraes, R.C. Montenegro, J.D. Yoneda, et al., Synthesis and anticancer activity of (E)-2-benzothiazole hydrazones, *Eur. J. Med. Chem.* 86 (2014) 12–16. doi:10.1016/j.ejmech.2014.08.039.
- [104] S.R. Girish, V.K. Revankar, V.B. Mahale, Oxomolybdenum (V) complexes of 2-benzothiazolyl hydrazones, *Transit. Met. Chem.* 21 (1996) 401–405.
- [105] K.L. Rinehart, Antitumor compounds from tunicates, *Med. Res. Rev.* 20 (2000) 1–27. doi:10.1002/(SICI)1098-1128(200001)20:1<1::AID-MED1>3.0.CO;2-A.
- [106] C.M. Rath, B. Janto, J. Earl, A. Ahmed, F.Z. Hu, L. Hiller, et al., Meta-omic Characterization of the Marine Invertebrate Microbial Consortium That Produces the Chemotherapeutic Natural Product ET-743, *ACS Chem. Biol.* 6 (2011) 1244–1256. doi:10.1021/cb200244t.

- [107] E.L. Cooper, D. Yao, Diving for drugs: tunicate anticancer compounds, *Drug Discov. Today*. 17 (2012) 636–648. doi:10.1016/j.drudis.2012.02.006.
- [108] R.G. Pearson, Hard and Soft Acids and Bases, *J. Am. Chem. Soc.* 85 (1963) 3533–3539. doi:10.1021/ja00905a001.
- [109] R.G. Pearson, Acids and bases, *Science*. 151 (1966) 172–177. doi:10.1126/science.151.3707.172.
- [110] K.L. Haas, K.J. Franz, Application of Metal Coordination Chemistry To Explore and Manipulate Cell Biology, *Chem. Rev.* 109 (2009) 4921–4960. doi:10.1021/cr900134a.
- [111] É.A. Enyedy, É. Zsigó, N.V. Nagy, C.R. Kowol, A. Roller, B.K. Keppler, et al., Complex-Formation Ability of Salicylaldehyde Thiosemicarbazone towards ZnII, CuII, FeII, FeIII and GaIII Ions, *Eur. J. Inorg. Chem.* 2012 (2012) 4036–4047. doi:10.1002/ejic.201200360.
- [112] P.J. Jansson, C.L. Hawkins, D.B. Lovejoy, D.R. Richardson, The iron complex of Dp44mT is redox-active and induces hydroxyl radical formation: An EPR study, *J. Inorg. Biochem.* 104 (2010) 1224–1228. doi:10.1016/j.jinorgbio.2010.07.012.
- [113] Y. Yu, D.S. Kalinowski, Z. Kovacevic, A.R. Sifakas, P.J. Jansson, C. Stefani, et al., Thiosemicarbazones from the Old to New: Iron Chelators That Are More Than Just Ribonucleotide Reductase Inhibitors, *J. Med. Chem.* 52 (2009) 5271–5294. doi:10.1021/jm900552r.
- [114] G.R. Fulmer, A.J.M. Miller, N.H. Sherden, H.E. Gottlieb, A. Nudelman, B.M. Stoltz, et al., NMR Chemical Shifts of Trace Impurities: Common Laboratory Solvents, Organics, and Gases in Deuterated Solvents Relevant to the Organometallic Chemist, *Organometallics*. 29 (2010) 2176–2179. doi:10.1021/om100106e.
- [115] J.K. Seydel, K.-J. Schaper, Substituierte 2-Acylpyridin- $\alpha$ -(N)-hetarylhydrazone sowie diese enthaltende Arzneimittel, DE3716131A1, 1987.

[116] H. Mueller, M.U. Kassack, M. Wiese, Comparison of the Usefulness of the MTT, ATP, and Calcein Assays to Predict the Potency of Cytotoxic Agents in Various Human Cancer Cell Lines, *J. Biomol. Screen.* 9 (2004) 506–515.

doi:10.1177/1087057104265386.

[117] I. GraphPad Software, GraphPad Prism, GraphPad Software, Inc., 2007.

[www.graphpad.com](http://www.graphpad.com).

**Captions for Schemes and Figures:**

**Scheme 1.** Synthesis of different Schiff bases starting from the preparation of thiosemicarbazides **C-1** ( $R^1$ :  $OCH_3$ ), **C-2** ( $R^1$ :  $CH_3$ ), **C-3** ( $R^1$ :  $NO_2$ ), or 2-hydrazinobenzothiazole, respectively. Reaction conditions: a: MeOH, stirring at rt; b: EtOH, HCl or HOAc catalysis, refluxing.  $X = N$  for compound series **2** and **5**;  $X = C-OH$  for compound series **3** and **6**. Substituents are  $R^1$ :  $CH_3$ ,  $OCH_3$  or  $NO_2$ ;  $R^2$ : H,  $CH_3$ ,  $R^3$ : H,  $OCF_3$ . Further compounds listed in Figure 2 were commercially available and purchased to complement the library.

**Figure 1.** Library design. The five molecules shown in the upper 3 panels possess variable MDR-selective toxicity and served as a starting point for the library design around isatin- $\beta$ -Thiosemicarbazones (TSC, box I), picolinylidene TSCs (box II), salicylidene TSCs (box III), arylhydrazones (box IV), picolinylidene hydrazinobenzothiazoles (box V), salicylidene hydrazinobenzothiazoles (box VI), as well as molecules with combined chemical entities (box VII). Chelators with ONS, NNS and NNN donor atoms are shown in red, blue and green boxes, respectively; donor atoms of example ligands are highlighted.

**Figure 2.** Library design. Overview of synthesized and purchased picolinylidene TSCs (box II), the acetaniline TSC **2p**, salicylidene TSCs (box III), arylhydrazones (box IV), picolinylidenehydrazinobenzothiazoles (box V), the acetaniline-hydrazinebenzothiazole **5d**, salicylidene-hydrazinobenzothiazoles (box VI) and molecules with combined chemical entities (box VII). Chelators with ONS, NNS and NNN donor atoms are shown in red, blue and green boxes, respectively.

**Figure 3.** Confirmation of MDR selective activity of isatin- $\beta$ -thiosemicarbazones. A-C: Dose response curves in absence (black) and presence (grey) of the P-gp inhibitor Tariquidar (1  $\mu$ M), obtained from 2 to 4 independent experiments of MTT assays on MES-SA (open squares) and MES-SA/Dx5 (filled squares) cells for A: Triapine, B: **1a** (NSC73306) and C: **1d**. D: Selectivity ratios of the obtained IC<sub>50</sub> values on P-gp (+) and (-) cells for the investigated isatin- $\beta$ -thiosemicarbazones; black: MES-SA/Dx5 vs. MES-SA cells, grey filled: MES-SA/Dx5 vs. MES-SA cells in presence of 1  $\mu$ M TQ, blue: KB-V1 vs. KB-3-1 cells, green: A2780adr vs. A2780. Significance of the difference between P-gp (+) and P-gp (-) cells was calculated using paired t-tests and is given as \*:  $p \leq 0.05$ , \*\*:  $p \leq 0.01$ , \*\*\*:  $p \leq 0.001$ , \*\*\*\*:  $p \leq 0.0001$ . E: P-gp negative fraction of MES-SA/Dx5 cells (as determined by the Calcein AM assay, see *Methods* [67]) at the beginning of the experiment (t=0), after long-term culture without treatment (contr) or treated with the IC<sub>20</sub> concentrations of **1a**, **1c** or **1d**. F-H: Immunocytochemical staining of cells. P-gp expression (MRK-16, red) of MES-SA/Dx5 cells (G) is restored to baseline levels (MES-SA cells, F) after 5 rounds of treatment with **1d** (H). Nuclei are stained with DAPI (blue); bar=20 micrometers.

**Figure 4.** SAR matrix of picolinylidene Schiff bases. Biodata was obtained using mCherry transfected MES-SA and MES-SA/Dx5 cells, average pIC<sub>50</sub> values of three independent experiments are shown with the color coding as indicated.

**Figure 5.** Effect of imino methylation on toxicity. Pairwise comparison of pIC<sub>50</sub> values from MMPs of chelators containing NNS (A) and NNN (B) donor atom sets obtained in A2780wt (open circles), A2780adr (filled circles), KB-3-1 (open triangles), KB-V1 (filled triangles), MES-SA (open squares), MES-SA/Dx5 (filled). Cyan: **2f** vs. **2g**, green: **4a** vs. **4b**, blue: **5a** vs. **5b**, bordeaux: **2n** vs. **2o**, pink: **2l** vs. **2m**, orange: **4e** vs. **4f**, red: **4g** vs. **4h**, (see Table S3 – S6

for details). **C**: Box and Whiskers plot of toxicity data on MES-SA-mCh and MES-SA/Dx5-mCh cells comparing NNN and NNS chelators with (blue) and without (cyan) methylation at the imino carbon ( $p=0.045$ ).

**Figure 6.** Structure-activity relationship matrix (SARM). Average  $pIC_{50}$  values of at least three independent experiments are shown for the A2780, KB and MES-SA cell pairs according to the arrangement shown in the inset. In general, data are obtained by MTT assays, those compounds marked with an asterisk were measured by the fluorescent cytotoxicity assay only. Data for **4a-c** are taken from Pape et al. [13].

**Figure 7.** Toxicity of picolinylidene (class V) and salicylidene (class VI) hydrazinobenzothiazole ligands. Biodata was obtained using mCherry transfected MES-SA and MES-SA/Dx5 cells,  $pIC_{50}$  values are shown with the color coding as indicated.

**Figure 8.** Influence of donor atom sets on toxicity: **A**: pairwise comparison of  $pIC_{50}$  values from matched molecular pairs (MMP) with ONS and NNS donor sets obtained in A2780wt (open circles), A2780adr (filled circles), KB-3-1 (open triangles), KB-V1 (filled triangles), MES-SA (open squares), MES-SA/Dx5 (filled squares). Different colors indicate the respective compound pairs: Cyan: **6a** vs. **5a**, green: **6b** vs. **5b**, blue: **3c** vs. **2f**, purple: **3d** vs. **2g**, orange: **3a** vs. **2a**, pink: **3e** vs. **2m** (For details, see Tables S3 - S6). **B**: Comparison of overall toxicity data of ONS (red), NNS (blue) and NNN (green) chelators with and without MMPs. Data from mCherry fluorescence measurements using MES-SA and MES-SA/Dx5 cells are shown (\*\* $p \leq 0.001$ , \*\*\*\* $: p \leq 0.0000001$ ). **C**: activity of ONS (red), NNS (blue) and NNN (green) chelators with and without MMPs in P-gp (+) and P-gp (-) cells, averaged over all investigated cell lines and assays.

**Figure 9.** Effect of the ONS and NNS donor atoms on toxicity against the NCI60 cell panel. Substructure search in the DTP drug database performed for NNS (A) or ONS (B) chelator scaffolds retrieved 946 and 389 search results, respectively. Biodata was available for 218 NNS chelators, 39 NNS compounds without chelating properties, 32 metal binding NNS chelators, 34 ONS chelators, 33 non-chelating ONS compounds and 29 ONS-metal complexes (see Figure S12). C: Pairwise comparison of cytotoxic activity of matched molecular ONS and NNS donor chelator pairs across the NCI60 cell panel. Structures of the compounds are shown below the graph (data for X = C-OH (red) or N (blue)). NSC95678 contains both binding options (purple). D: Average toxicity of the compounds identified by the substructure search ( $\text{pIC}_{50}$  values averaged over the 60 cell lines).

**Supporting Information:**

Table S1: Reported MDR selective isatin- $\beta$ -thiosemicarbazones identified in the DTP database [15]

Tables S2-S6: Predicted physicochemical properties and measured biological data of isatin  $\beta$ -TSCs (Table S2), pyridinecarbaldehyde TSCs (Table S3), salicylaldehyde TSCs (Table S4), arylhydrazones (Table S5) and hydrazinobenzothiazoles (Table S6).

Tables S7-S8: Correlation of toxic activity to physicochemical properties of pyridinylidene Schiff bases from Figure 4 (Table S7), and hydrazinobenzothiazoles from Figure 7B (Table S8).

Figure S1: Comparison of toxicity in cancerous cell lines vs. non-cancerous HFF fibroblast cells.

Figure S2: Comparison of MTT and mCherry assay results on MES-SA and MES-SA/Dx5 cells using 35 different compounds.

Figure S3-S7: Box and Whiskers plots of selectivity ratios (SR) of isatin  $\beta$ -TSCs (Figure S3 A), pyridinecarbaldehyde TSCs (Figure S4), salicylaldehyde TSCs (Figure S5), arylhydrazones (Figure S6) and hydrazinobenzothiazoles (Figure S7). Cell growth and schedule for long term treatment with IC<sub>20</sub> concentration of **1d** (Figure S3 B) and histograms characterizing the cells with Calcein AM assay (Figure S3 C-F).

Figure S8: Effect of Tariquidar on toxicity of investigated compounds.

Figure S9: Comparison of toxicity data for chelators with and without imino-methylation obtained in P-gp positive vs. negative cell lines.

Figure S11: Comparison of toxicity data for chelators with different donor atom sets obtained in P-gp positive vs. negative cell lines.

Figure S12: Flowchart of the identification of NNS (A) and ONS (B) donor chelators in the DTP database. C: example for a non-chelating NNS molecule NSC656776; D: outstandingly toxic non chelating ONS molecules.

Figure S13: Refinement of search results from Figure F with respect to imino carbon substitution.



Figures S14-S19: Representative  $^1\text{H}$  (A) and  $^{13}\text{C}$  (B) spectra of compounds **2c**, **2j**, **3b**, **5c**, **6b**, and **7c**.

ACCEPTED MANUSCRIPT

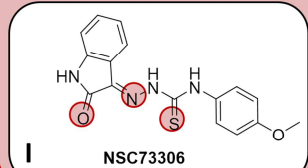
**Table 1.** Compounds showing increased toxicity in MDR cells.

Selectivity ratios (SR) were determined as the fraction of IC<sub>50</sub> values obtained in P-gp negative vs. positive cells. The median of SR values obtained in at least 3 independent experiments (see Figures S2 – S6 for experimental data) is given for the respective test systems. The effect is considered P-gp dependent, if inhibition of the transporter (as achieved by TQ coadministration, see Figure S7) abolishes MDR-selective toxicity

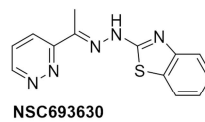
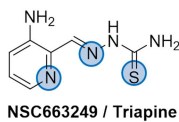
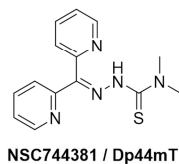
Compound	Cell lines	median SR <sup>[b]</sup>	Effect of P-gp inhibition on MDR selectivity
<b>1a</b>	MES-SA / MES-SA/Dx5 <sup>[a]</sup>	1.87	yes
	MES-SA / MES-SA/Dx5 <sup>[b]</sup>	3.17	yes
	KB-3-1 / KB-V1	2.04	yes (not shown)
	A2780 / A2780adr	1.60	yes (not shown)
<b>1b</b>	MES-SA / MES-SA/Dx5 <sup>[a]</sup>	2.31	yes
	MES-SA / MES-SA/Dx5 <sup>[b]</sup>	3.29	yes
<b>1c</b>	MES-SA / MES-SA/Dx5 <sup>[a]</sup>	1.87	no
	MES-SA / MES-SA/Dx5 <sup>[b]</sup>	3.1	yes
<b>1d</b>	MES-SA / MES-SA/Dx5 <sup>[a]</sup>	1.77	yes
	MES-SA / MES-SA/Dx5 <sup>[b]</sup>	3.55	yes
	KB-3-1 / KB-V1	1.82	yes (not shown)
	A2780 / A2780adr	2.98	yes (not shown)
<b>1e</b>	MES-SA / MES-SA/Dx5 <sup>[a]</sup>	1.44	yes
	MES-SA / MES-SA/Dx5 <sup>[b]</sup>	2.42	yes
<b>2c</b>	MES-SA / MES-SA/Dx5 <sup>[a]</sup>	22.59	no
	MES-SA / MES-SA/Dx5 <sup>[b]</sup>	4.54	no
<b>2f</b>	MES-SA / MES-SA/Dx5 <sup>[a]</sup>	4.55	no
<b>2g</b>	MES-SA / MES-SA/Dx5 <sup>[a]</sup>	6.25	no
	KB-3-1 / KB-V1	1.15	no (not shown)
<b>3a</b>	MES-SA / MES-SA/Dx5 <sup>[b]</sup>	2.23	no
<b>4b</b>	MES-SA / MES-SA/Dx5 <sup>[a]</sup>	2.62	no (not shown)
	A2780 / A2780adr	4.33	no (not shown)
<b>4c</b>	MES-SA / MES-SA/Dx5 <sup>[a]</sup>	1.41	no
	A2780 / A2780adr	2.03	no (not shown)
<b>5a</b>	MES-SA / MES-SA/Dx5 <sup>[a]</sup>	1.41	-
<b>5b</b>	MES-SA / MES-SA/Dx5 <sup>[a]</sup>	17.58	no
<b>5c</b>	MES-SA / MES-SA/Dx5 <sup>[a]</sup>	1.68	-
<b>5d</b>	MES-SA / MES-SA/Dx5 <sup>[a]</sup>	1.64	-
	MES-SA / MES-SA/Dx5 <sup>[b]</sup>	2.41	-
<b>6a</b>	MES-SA / MES-SA/Dx5 <sup>[a]</sup>	2.04	no
	MES-SA / MES-SA/Dx5 <sup>[b]</sup>	7.18	yes
<b>6b</b>	MES-SA / MES-SA/Dx5 <sup>[a]</sup>	1.91	no
	MES-SA / MES-SA/Dx5 <sup>[b]</sup>	1.90	no
<b>6d</b>	MES-SA / MES-SA/Dx5 <sup>[b]</sup>	4.71	no
<b>6e</b>	MES-SA / MES-SA/Dx5 <sup>[b]</sup>	5.65	no

[a] MTT. [b] mCherry

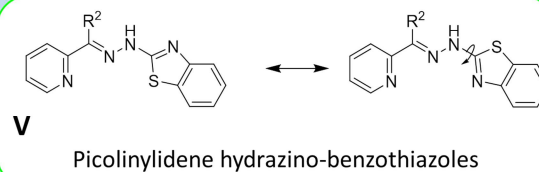
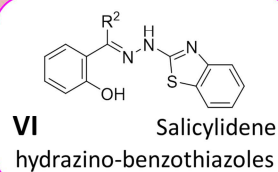
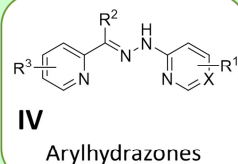
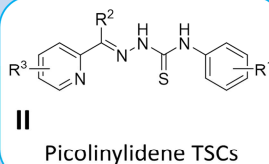
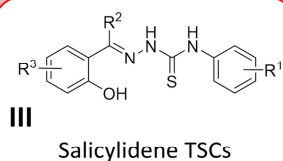
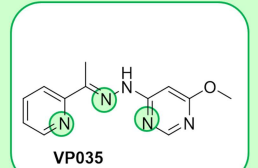
## ONS donor chelators



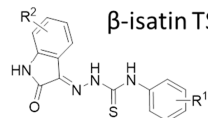
## NNS donor chelators



## NNN donor chelators

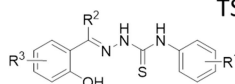
**VII** Combination of chemical entities

ACCEPTED

I  $\beta$ -isatin TSCs

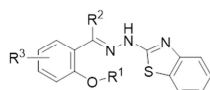
	R1	R2
1a	4-OMe	H
1b	4-OMe	5-OCF <sub>3</sub>
1c	4-Me	H
1d	4-NO <sub>2</sub>	H
1e	3-CF <sub>3</sub>	H

## III Salicylidene TSCs



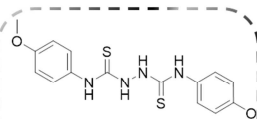
	R1	R2	R3
3a	H	H	H
3b	4-OMe	H	H
3c	4-Me	H	H
3d	4-Me	Me	H
3e	3-CF <sub>3</sub>	H	H
3f	3-CF <sub>3</sub>	H	4-NO <sub>2</sub>
3g	2-CF <sub>3</sub>	H	4-NO <sub>2</sub>

## VI Salicylidene hydrazino-benzothiazoles



	R1	R2	R3
6a	H	H	H
6b	H	Me	H
6c	H	H	4-OMe
6d	H	Me	4-OMe
6e	H	H	4-Me
6f	H	H	4-NO <sub>2</sub>
6g	Me	H	H

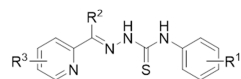
## VII



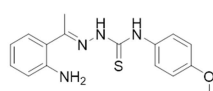
Dimerization of  
NSC73307

7a

## II Picolinylidene TSCs

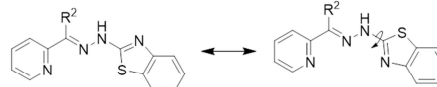


	R1	R2	R3
2a	H	H	H
2b	H	Me	H
2c	4-OMe	Me	H
2d	4-OMe	H	2-Me
2e	4-OMe	H	3-Et
2f	4-Me	H	H
2g	4-Me	Me	H
2h	3-Me	Me	H
2i	2-Me	Me	H
2j	4-NO <sub>2</sub>	H	H
2k	4-NO <sub>2</sub>	H	3-Et
2l	3-CF <sub>3</sub>	H	H
2m	3-CF <sub>3</sub>	Me	H
2n	2-CF <sub>3</sub>	H	H
2o	2-CF <sub>3</sub>	Me	H

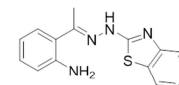


Acetaniline TSC 2p

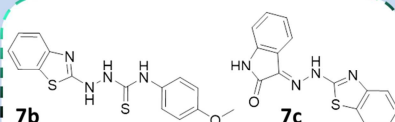
## V Picolinylidene hydrazino-benzothiazoles



	R2	R3
5a	H	
5b	Me	
5c	H	Et

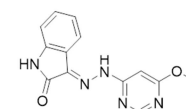
Acetaniline-  
hydrazino-benzothiazole 5d

## Combination of chemical entities



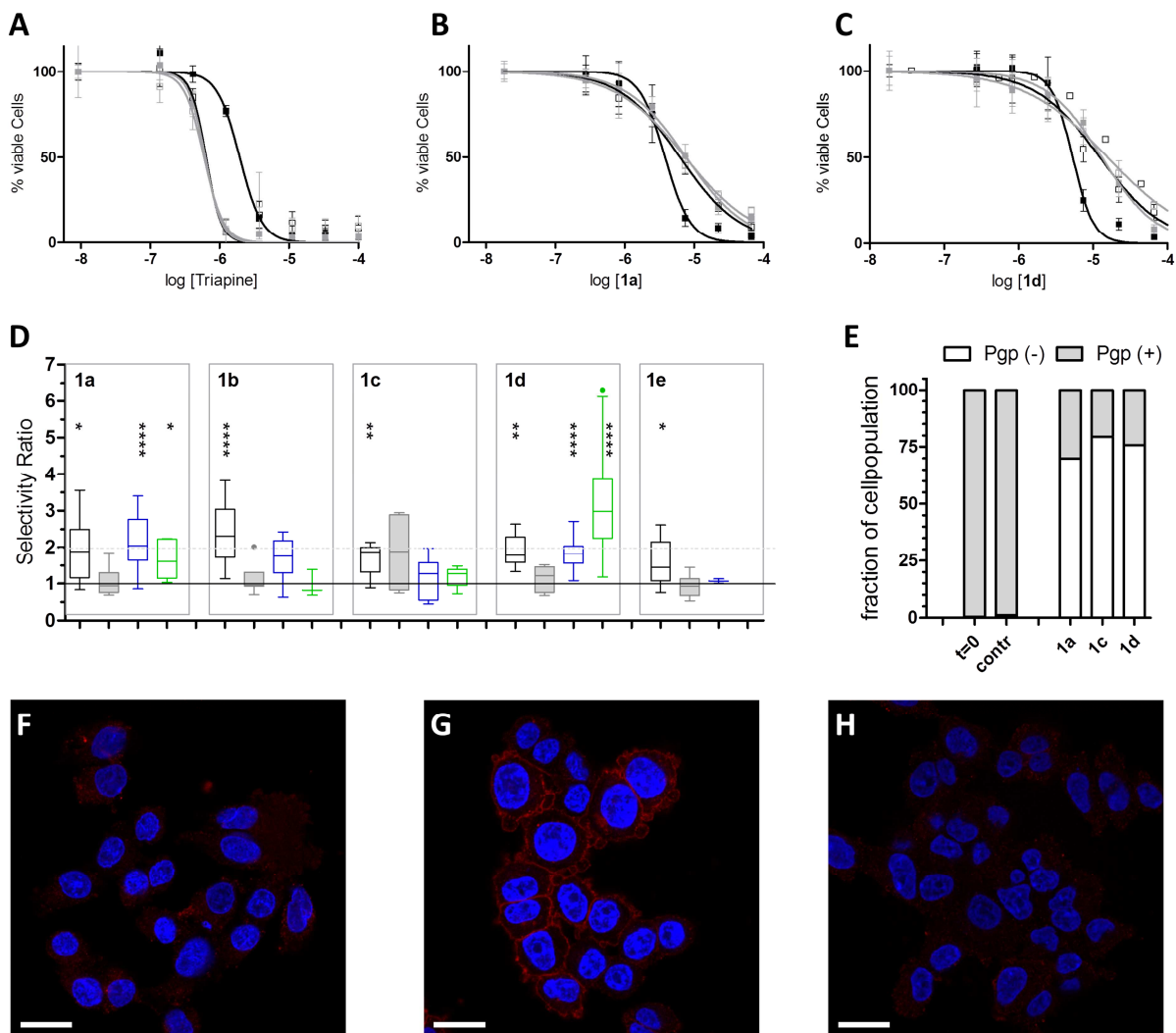
7b

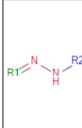
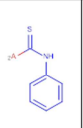
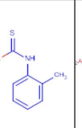
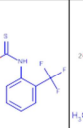
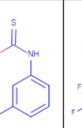
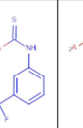
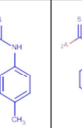
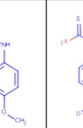
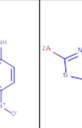
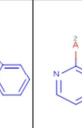
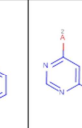
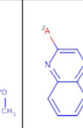
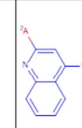
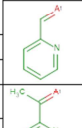
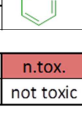
7c

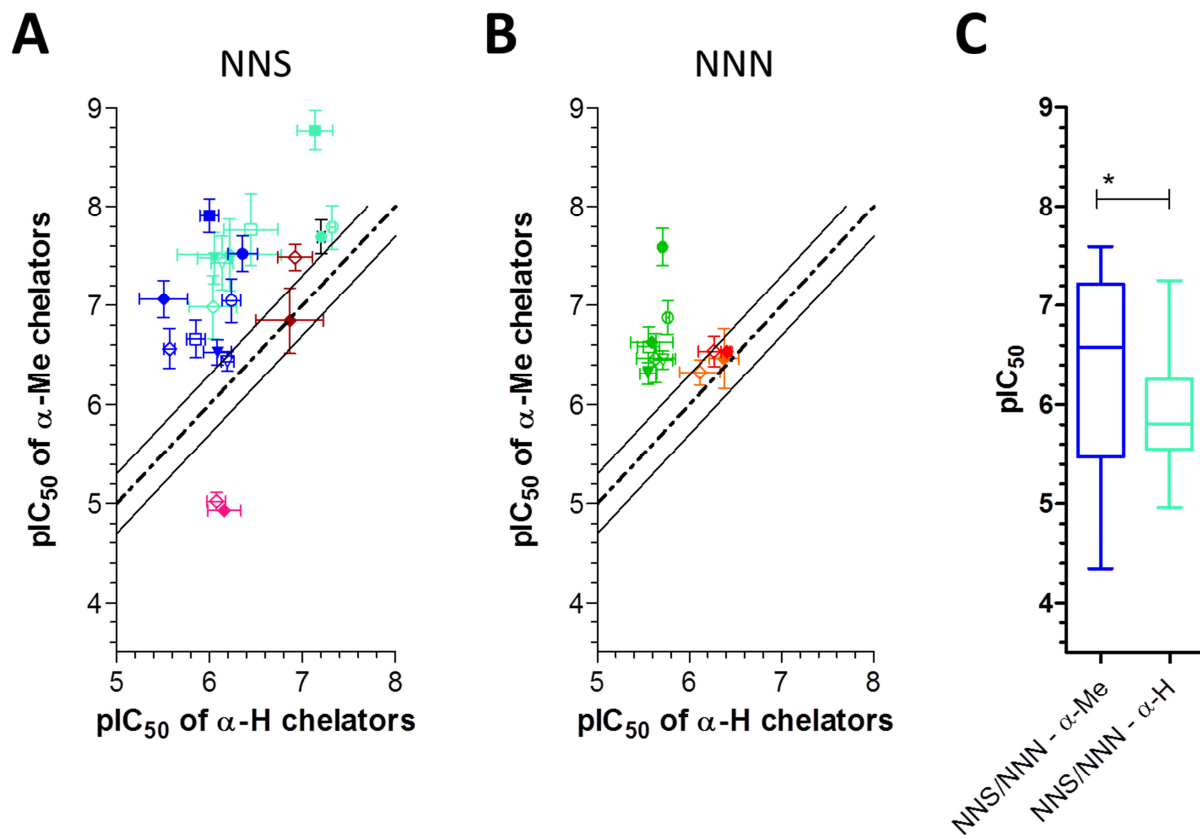
Combination of NSC73306 with  
hydrazino-benzothiazoles

7d

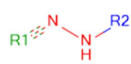
Combination of NSC73306  
with pyrimidinylhydrazone

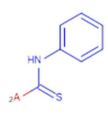
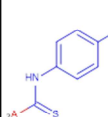
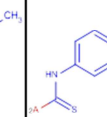
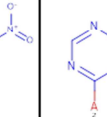
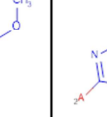
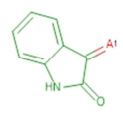
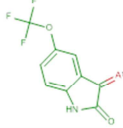
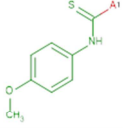
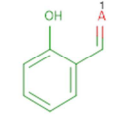
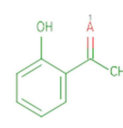
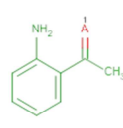
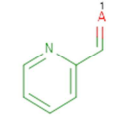
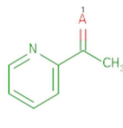
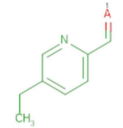
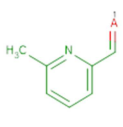


														
pIC <sub>50</sub>		<b>2a</b>		<b>2n</b>		<b>2l</b>	<b>2f</b>		<b>2j</b>	<b>5a</b>		<b>4a</b>	<b>4e</b>	<b>4g</b>
MES-SA		6,16		6,92		6,08	6,12		5,57	5,57		5,63	6,11	6,27
Dx5		6,25		6,86		6,16	6,25		5,56	5,51		5,59	6,37	6,40
pIC <sub>50</sub>		<b>2b</b>	<b>2i</b>	<b>2o</b>	<b>2h</b>	<b>2m</b>	<b>2g</b>	<b>2c</b>		<b>5b</b>	<b>4d</b>	<b>4b</b>	<b>4f</b>	<b>4h</b>
MES-SA		n.tox.	7,53	7,49	7,50	5,02	7,38	6,64		6,62	7,11	6,47	6,32	6,54
Dx5		n.tox.	7,06	6,85	7,21	4,93	7,59	7,24		7,08	7,23	6,63	6,46	6,53
pIC <sub>50</sub>	<b>n.tox.</b>	<b>4,00</b>	<b>4,50</b>	<b>5,00</b>	<b>5,50</b>	<b>6,00</b>	<b>6,50</b>	<b>7,00</b>	<b>7,50</b>	<b>8,00</b>	<b>8,50</b>			
IC <sub>50</sub>	not toxic	100.0 μM	31.6 μM	10 μM	3.2 μM	1.0 μM	316.2 nM	100.0 nM	31.6 nM	10 nM	3.2 nM			



R1

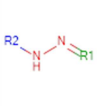
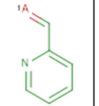
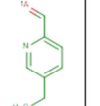
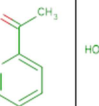
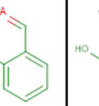
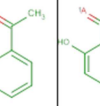
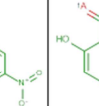
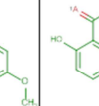
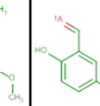
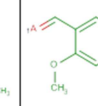

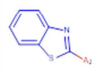
R2 

								
ONS / ONN			<b>1a</b>	<b>1c</b>	<b>1d</b>	<b>7d</b>	<b>7c</b>	
			5,13 5,33	5,02 5,05	4,61 5,05	n.tox. n.tox.		
			5,12 5,40	5,38 5,40	5,11 5,35	4,26 4,17		
			<b>1b</b>					
			5,49 5,45					
			5,21 5,41					
			5,24 5,59					
			<b>7a</b>				<b>7b</b>	
			n.tox. n.tox.				n.tox. n.tox.	
							n.tox. n.tox.	
NNS / NNN		<b>3a *</b>	<b>3b</b>	<b>3c</b>			<b>6a</b>	
			5,27 5,16	5,30 5,22			5,51 5,23	
			5,30 5,30	5,48 5,46			4,80 4,93	
		4,94 5,32	5,42 5,46	5,43 5,39			4,63 5,02	
				<b>3d *</b>			<b>6b</b>	
				5,01 5,36			5,08 5,01	
							4,86 4,94	
							4,91 5,28	
				<b>2p</b>				<b>5d</b>
				5,37 5,31				
			4,69 4,65					
			4,98 5,10				4,35 4,56	
		<b>2a *</b>		<b>2f</b>	<b>2j</b>	<b>4a</b>	<b>5a</b>	
				7,32 7,20	6,21 5,87	5,76 5,71	6,24 6,35	
				6,14 6,05	5,99 5,75	5,72 5,55	6,19 6,09	
		6,16 6,25		6,44 7,14	5,59 5,75	5,56 5,61	5,85 6,00	
		<b>2b *</b>	<b>2c</b>	<b>2g</b>		<b>4b</b>	<b>5b</b>	
			7,34 7,55	7,79 7,69		6,88 7,59	7,05 7,52	
			6,16 5,98	7,43 7,48		6,45 6,31	6,43 6,53	
		n.tox. n.tox.	6,47 7,85	7,77 8,77		6,58 7,04	6,66 7,91	
			<b>2e</b>		<b>2k</b>	<b>4c</b>	<b>5c</b>	
						5,89 6,21	6,09 6,23	
					5,10 5,05	5,91 5,81	6,03 5,94	
			6,38 7,20		4,97 5,09	5,82 5,96	5,50 5,73	
			<b>2d *</b>					
			5,33 5,38					

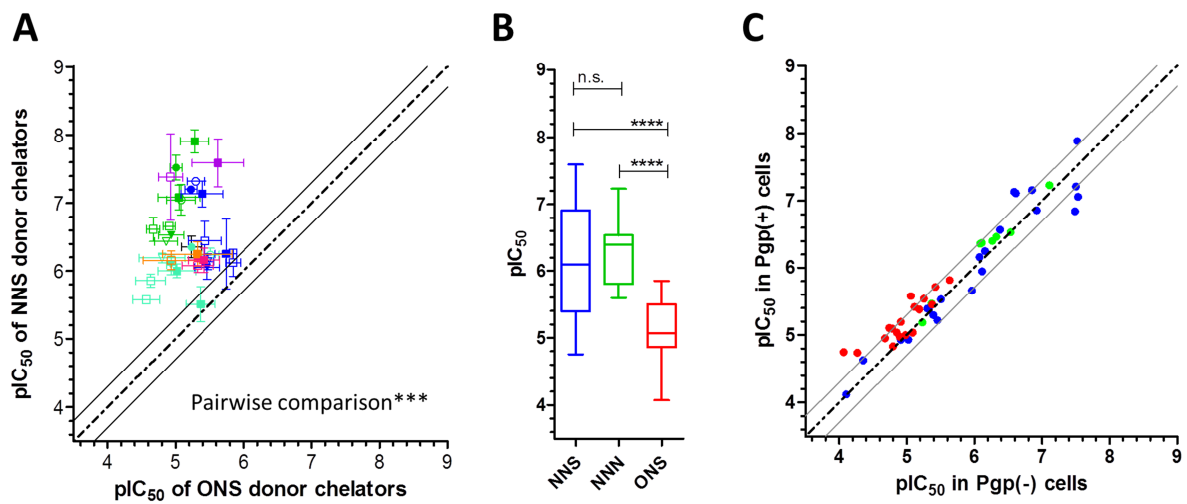
cell lines	
A2780	A2780adr
KB-3-1	KB-v1
messia	dx5

pIC <sub>50</sub>	IC <sub>50</sub>
n.tox.	not toxic
4,00	100.0 μM
4,50	31.6 μM
5,00	10 μM
5,50	3.2 μM
6,00	1.0 μM
6,50	316.2 nM
7,00	100.0 nM
7,50	31.6 nM
8,00	10 nM
8,50	3.2 nM

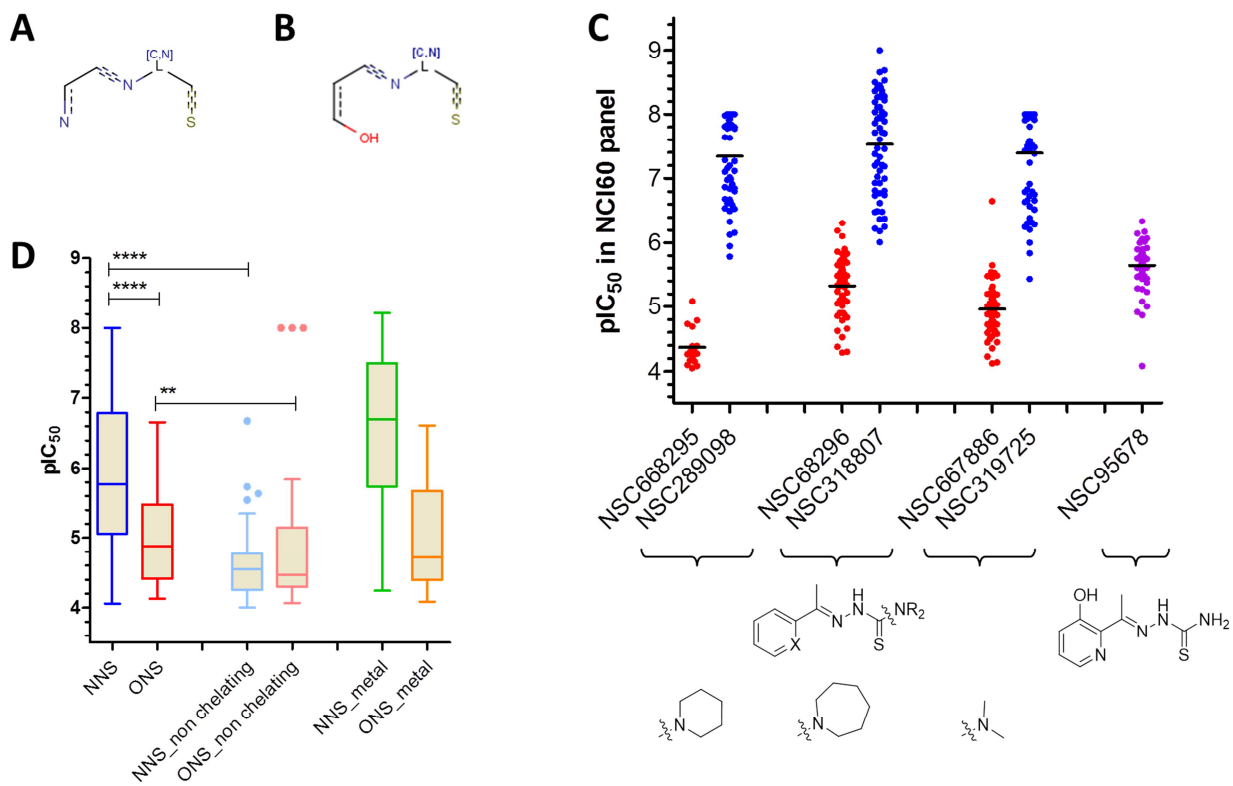


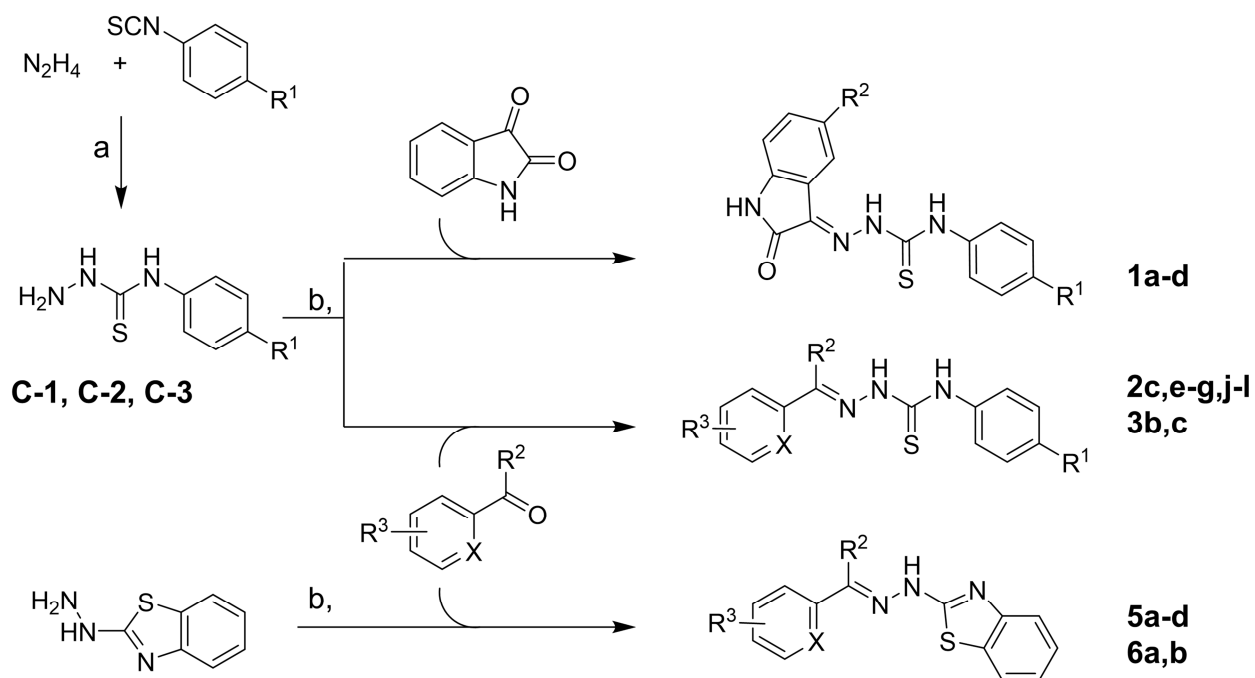
											
pIC <sub>50</sub>		<b>5a</b>	<b>5c</b>	<b>5b</b>	<b>6a</b>	<b>6b</b>	<b>6f</b>	<b>6c</b>	<b>6d</b>	<b>6e</b>	<b>6g</b>
MES-SA		5,57	5,37	6,62	4,57	4,67	5,42	4,88	4,30	4,07	n.tox.
Dx5		5,51	5,45	7,08	5,37	5,05	5,73	5,03	4,85	4,86	n.tox.
pIC <sub>50</sub>	n.tox.	4,00	4,50	5,00	5,50	6,00	6,50	7,00	7,50	8,00	8,50
IC <sub>50</sub>	not toxic	100.0 μM	31.6 μM	10 μM	3.2 μM	1.0 μM	316.2 nM	100.0 nM	31.6 nM	10 nM	3.2 nM

ACCEPTED MANUSCRIPT



ACCEPTED MANUSCRIPT





**Highlights**

- A focused library of ONS, NNS and NNN donor chelators was designed and synthesized
- Thiosemicarbazones, arylhydrazones and hydrazinobenzothiazoles were investigated
- In vitro antiproliferative activity was tested in sensitive and MDR cancer cells
- Molecular features influencing the toxicity of anticancer chelators were identified